



NAVAL POSTGRADUATE SCHOOL

MONTEREY, CALIFORNIA

THESIS

**TECHNIQUE FOR GEOLOCATION OF EMI EMITTERS
BY O3B SATELLITES**

by

James P. Connolly

June 2016

Thesis Advisor:
Second Reader:

Charles M. Racoosin
Herschel H. Loomis

Approved for public release; distribution is unlimited

THIS PAGE INTENTIONALLY LEFT BLANK

REPORT DOCUMENTATION PAGE			<i>Form Approved OMB No. 0704-0188</i>	
Public reporting burden for this collection of information is estimated to average 1 hour per response, including the time for reviewing instruction, searching existing data sources, gathering and maintaining the data needed, and completing and reviewing the collection of information. Send comments regarding this burden estimate or any other aspect of this collection of information, including suggestions for reducing this burden, to Washington headquarters Services, Directorate for Information Operations and Reports, 1215 Jefferson Davis Highway, Suite 1204, Arlington, VA 22202-4302, and to the Office of Management and Budget, Paperwork Reduction Project (0704-0188) Washington DC 20503.				
1. AGENCY USE ONLY (Leave blank)		2. REPORT DATE June 2016		3. REPORT TYPE AND DATES COVERED Master's thesis
4. TITLE AND SUBTITLE TECHNIQUE FOR GEOLOCATION OF EMI EMITTERS BY O3B SATELLITES			5. FUNDING NUMBERS	
6. AUTHOR(S) James P. Connolly				
7. PERFORMING ORGANIZATION NAME(S) AND ADDRESS(ES) Naval Postgraduate School Monterey, CA 93943-5000			8. PERFORMING ORGANIZATION REPORT NUMBER	
9. SPONSORING / MONITORING AGENCY NAME(S) AND ADDRESS(ES) N/A			10. SPONSORING / MONITORING AGENCY REPORT NUMBER	
11. SUPPLEMENTARY NOTES The views expressed in this thesis are those of the author and do not reflect the official policy or position of the Department of Defense or the U.S. Government. IRB Protocol number ____N/A____.				
12a. DISTRIBUTION / AVAILABILITY STATEMENT Approved for public release; distribution is unlimited			12b. DISTRIBUTION CODE	
13. ABSTRACT (maximum 200 words) This thesis investigates how and to what effectiveness the O3b commercial satellite constellation could be used for geolocation of Ka-band EMI sources in support of the DOD. Review of commonly used geolocation techniques for suitability and comparison of those with the O3b constellation characteristics shows that a new method of geolocation is necessary and possible. A method using the Doppler effect with frequency data from a single antenna was then created that is compatible with O3b. This method uses the received frequency of the jammer over time to detect the base frequency, and then compares the received frequency to that of simulated emitters at known locations in order to provide a geolocation for EMI emitters. This was modeled to be accurate within 16 km throughout O3b's service area. This level of accuracy would provide the ability to mitigate the interference or decrease a search area for assets with higher capabilities in order to increase their efficiency of tasking/use. This method is of further benefit to the DOD due to its potential to be low cost, be maintained as an organic capability by the units, and decrease the time necessary to reach a conclusion when working through the Joint Spectrum Interference Resolution process.				
14. SUBJECT TERMS geolocation, interference, SATCOM, O3b			15. NUMBER OF PAGES 103	
			16. PRICE CODE	
17. SECURITY CLASSIFICATION OF REPORT Unclassified	18. SECURITY CLASSIFICATION OF THIS PAGE Unclassified	19. SECURITY CLASSIFICATION OF ABSTRACT Unclassified	20. LIMITATION OF ABSTRACT UU	

THIS PAGE INTENTIONALLY LEFT BLANK

Approved for public release; distribution is unlimited

**TECHNIQUE FOR GEOLOCATION OF EMI EMITTERS BY O3B
SATELLITES**

James P. Connolly
Captain, United States Marine Corps
B.S., University of Maine, 2008

Submitted in partial fulfillment of the
requirements for the degree of

MASTER OF SCIENCE IN SPACE SYSTEMS OPERATIONS

from the

**NAVAL POSTGRADUATE SCHOOL
June 2016**

Approved by: Charles M. Racoosin
Thesis Advisor

Herschel H. Loomis
Second Reader

Rudolf Panholzer
Chair, Space Systems Academic Group

THIS PAGE INTENTIONALLY LEFT BLANK

ABSTRACT

This thesis investigates how and to what effectiveness the O3b commercial satellite constellation could be used for geolocation of Ka-band EMI sources in support of the DOD. Review of commonly used geolocation techniques for suitability and comparison of those with the O3b constellation characteristics shows that a new method of geolocation is necessary and possible. A method using the Doppler effect with frequency data from a single antenna was then created that is compatible with O3b. This method uses the received frequency of the jammer over time to detect the base frequency, and then compares the received frequency to that of simulated emitters at known locations in order to provide a geolocation for EMI emitters. This was modeled to be accurate within 16 km throughout O3b's service area. This level of accuracy would provide the ability to mitigate the interference or decrease a search area for assets with higher capabilities in order to increase their efficiency of tasking/use. This method is of further benefit to the DOD due to its potential to be low cost, be maintained as an organic capability by the units, and decrease the time necessary to reach a conclusion when working through the Joint Spectrum Interference Resolution process.

THIS PAGE INTENTIONALLY LEFT BLANK

TABLE OF CONTENTS

I.	INTRODUCTION.....	1
A.	SATELLITE COMMUNICATIONS OVERVIEW	2
B.	EMI AND JAMMING OVERVIEW	5
1.	Why EMI/Jamming Is an Issue for the DOD.....	6
2.	How Jamming Occurs	7
C.	CONCLUSION	10
II.	GEOLOCATION OF EMI SOURCES	13
A.	WHY FINDING EMI SOURCES IS IMPORTANT.....	13
B.	CURRENT GEOLOCATION TECHNIQUES OVERVIEW.....	13
1.	Multiple Satellite Methods	14
2.	Multiple Antenna Methods	17
3.	Single Antenna Methods.....	18
C.	WHY GEOLOCATING EMI SOURCES IN KA-BAND IS CHALLENGING	19
1.	Number of Satellites.....	19
2.	Antenna Gain and Beamwidth	20
D.	CONCLUSION	23
III.	O3B AND SUITABILITY FOR GEOLOCATION TECHNIQUE(S)	25
A.	CONSTELLATION DESIGN	25
B.	SATELLITE CHARACTERISTICS	25
C.	USEFUL CHARACTERISTICS FOR GEOLOCATION.....	27
D.	CONCLUSION	29
IV.	GEOLOCATION TECHNIQUE	31
A.	TECHNIQUE DEVELOPMENT.....	32
B.	MODELING.....	40
C.	ADDING COMPLEXITY.....	41
D.	CONCLUSION	50
V.	RESULTS, FUTURE WORK, AND CONCLUSIONS.....	51
A.	RESULTS	51
1.	Longitude LOP Results	53
2.	Latitude LOP Results	55
3.	Conclusion	57
B.	UTILITY OF THE GEOLOCATION METHOD.....	58

C.	FUTURE WORK	59
D.	CONCLUSION	60
APPENDIX A. SAMPLE DATA FOR USE IN MATLAB PROGRAM.....		63
APPENDIX B. MATLAB GEOLOCATION PROGRAM CODE		71
LIST OF REFERENCES		83
INITIAL DISTRIBUTION LIST		85

LIST OF FIGURES

Figure 1.	O3b Satellite Payload Antenna Pattern with Half-Power Beamwidth and Side Lobes.....	8
Figure 2.	Family of Hyperbolic TDOA Isochrons.	15
Figure 3.	TDOA and FDOA Contours.	17
Figure 4.	O3b Satellite Payload Antenna Receive Pattern.	26
Figure 5.	O3b Beam Coverage.	27
Figure 6.	Flat Non-rotating Earth Geolocation Geometry.	34
Figure 7.	Received Frequency as a Function of Emitter Relative Position.....	35
Figure 8.	Doppler Shift from Emitters Located ahead of Satellite.....	36
Figure 9.	Doppler Shift from Emitters Transiting abeam Satellite.	36
Figure 10.	Doppler Shift from Emitters Located behind Satellite.	37
Figure 11.	Received Frequency from EMI and Simulated Emitters.	39
Figure 12.	Graph for Interpolation of Cross-Track LOP.....	40
Figure 13.	Received Frequency Plot for EMI Emitter from STK Data.	43
Figure 14.	Received Frequency Plot Adjusted after Abeam Time Identified.	43
Figure 15.	Reference System.....	45
Figure 16.	Received Frequency Curves of Simulated Emitters at Various Latitude.	49
Figure 17.	Comparison of Received Frequency between EMI and Simulated Emitters.	49
Figure 18.	Graph for Interpolation of Latitude of EMI Emitter.....	50

THIS PAGE INTENTIONALLY LEFT BLANK

LIST OF TABLES

Table 1.	Sample Data Excerpt for Geolocation.	42
Table 2.	Actual and Estimated Emitter Locations—Emitter Located at Beam’s Boresight Latitude.	52
Table 3.	Actual and Estimated Emitter Locations—Beam’s Boresight 3°S of Emitter Latitude.	52
Table 4.	Actual and Estimated Emitter Locations—Beam’s Boresight 3°N of Emitter Latitude.	53
Table 5.	Longitude LOP Error Analysis.	54
Table 6.	Latitude LOP Error Analysis.	56
Table 7.	Magnitude of Error Summary for Latitude and Longitude.....	57
Table 8.	STK Generated Data for Emitter at 30°N 000°E.....	63

THIS PAGE INTENTIONALLY LEFT BLANK

LIST OF ACRONYMS AND ABBREVIATIONS

AOP	area of probability
BCA	beam coverage area
CEPT	European Conference of Postal and Telecommunications
CJCSM	Chairman of the Joint Chiefs of Staff Manual
dBW	decibel watt
DOD	Department of Defense
EC	Earth coverage
EM	electromagnetic
EMI	electromagnetic interference
EW	electronic warfare
GEO	geosynchronous orbit
GHz	gigahertz
GPS	Global Positioning System
HEO	highly elliptical orbit
HTS	high throughput satellite
Hz	hertz
ISR	intelligence, surveillance, reconnaissance
JSIR	Joint Spectrum Interference Resolution
LEO	low Earth orbit
LLA	latitude, longitude, altitude
MEO	medium Earth orbit
SATCOM	satellite communications
SIGINT	signals intelligence
SMAD	Space Mission Analysis and Design
STK	Systems Tool Kit
TT&C	tracking, telemetry and command
WGS	Wideband Global SATCOM

THIS PAGE INTENTIONALLY LEFT BLANK

ACKNOWLEDGMENTS

I would like to thank my thesis advisor, Charles Racoosin, for the extensive amount of time spent providing guidance for me not only for work on this thesis, but throughout my time working toward completion of this curriculum. There were many occasions on which I became “lost in the weeds” and needed some help in getting back on the correct path, which you always quickly provided. I greatly appreciate the time you spent and could not have completed this without you.

Thank you to my second reader, Herschel Loomis, for sharing your expertise in the field of geolocation and communications with me through various classes you taught and providing your inputs for this thesis. It has been a wonderful experience learning from such an experienced professor in the field.

I would also like to thank O3b Networks, particularly Ken Mentasti and J.J. Shaw, for their extensive support by providing information on the O3b satellites, including answering countless emails and questions, always thoroughly, quickly, and cheerfully.

Finally, I would like to thank my friends and family. Your support and encouragement is what enables me to accomplish everything that I do. Most of all, I thank my wife, Chelsea, for her continuous love and support during this time. She has had tremendous patience with the many long hours I spent on school work during these past two years, and especially in these last few months. She also created our wonderful son in only slightly more time than it took me to create this thesis, and is now a truly wonderful mother. I love you and baby Dan both very much!

THIS PAGE INTENTIONALLY LEFT BLANK

I. INTRODUCTION

The primary research question for this thesis was how, and to what effectiveness, could the O3b commercial satellite constellation be used for geolocation of Ka-band EMI sources in support of the DOD? There has been an increasing move of SATCOM users, including military, to the Ka-band in order to avoid congestion and support high data rates. The military also already relies heavily on commercial SATCOM to meet bandwidth requirements. Those tendencies, combined with the need for geolocation services in order to preserve the SATCOM capability, and the possibility that such services could be provided cheaply and directly to the user, made this an interesting research focus with great potential benefit to the DOD.

In breaking the primary research question into pieces and developing the subject, it is first important to develop what SATCOM EMI is and why it is an issue. These will be addressed in the remainder of Chapter I, following an overview of satellite communications.

Next, the case for why geolocation of the source of EMI is important must be made. Geolocation operations in the Ka-band present particular challenges that must be addressed as well. Following those issues, an overview of existing geolocation techniques must be made. The techniques' suitability for use will then be determined. These subsidiary topics will be covered in Chapter II.

A technique must then be chosen or developed and applied to the O3b constellation with its specific traits considered. As the O3b constellation is unique among communications constellations currently in use, its characteristics will be discussed in Chapter III.

The development or selection of a geolocation technique and characterization of the accuracy with which that method is able to perform geolocation of an interference source must be made. Chapter IV of this thesis will do that, with a different perspective on how to use Doppler shift as determined in the received frequency of the satellite. This

is evaluated for proof of concept as an alternative to existing methods for geolocation of EMI emitters.

Finally, in Chapter V, the usefulness of the suitable technique(s) for geolocation of EMI emitters is discussed with the emphasis on capability to mitigate the communications' interference and potential benefits to the DOD if O3b were to implement a geolocation of EMI emitter capability.

Chapter VI will address future work that could be done to improve the thesis by increasing the scope and utility, improving geolocation accuracy, or investigating alternative methods to address the research questions.

In limiting the scope of the thesis, emphasis was placed on finding a technique(s) for geolocation that preferably required a minimal number of satellites (ideally one), a minimum number of antennas (ideally one), and is a “passive” method—which is used in this case to mean it is only receiving signals. This thesis will be best understood by readers having a basic understanding of satellite communications (SATCOM) and orbital mechanics, as the underlying concepts used in techniques for geolocation of EMI emitters are dependent on the geometry and/or relative motion between an emitter (the EMI source) and the satellite (EMI receiver), and the motion/characteristics of radio waves.

A. SATELLITE COMMUNICATIONS OVERVIEW

The idea of satellite communications has existed since at least 1945, when Arthur C. Clarke was published discussing the use of satellites for transmitting television signals.¹ The idea of satellite communications provided a solution to the issue of our non-flat Earth preventing radio waves from reaching distant receivers. Arthur Clarke's idea was greatly expanded upon in the 1950s as AT&T took an interest and began work in earnest at making the idea a reality.² In 1957, Sputnik I was launched, not specifically with a communication orientation, but as the first man-made satellite an important leap

¹ David G. Whalen, “Communications Satellites Short History,” NASA History Division, November 30, 2010, <http://history.nasa.gov/satcomhistory.html>.

² Ibid.

forward in the quest for satellite communications.³ By the end of the 1950s, NASA had launched communication-oriented high-altitude balloons, which served as communications reflectors, and the U.S. Department of Defense (DOD) was researching developing active communications satellites.⁴ In the early 1960s, the first devoted communication satellite, TELSTAR, was launched.⁵ This was soon followed by other programs with RELAY, SYNCOM and EARLY BIRD all by the middle of the 1960s.⁶ Since then, satellite communications have grown tremendously and now exist in all major orbital regimes: low earth orbit (LEO), medium earth orbit (MEO), geosynchronous orbit (GEO), and highly elliptical orbit (HEO). Satellites are capable of serving customers globally and play a huge role in meeting communication needs for all, from individuals to companies to militaries.

Satellite communications are conducted by transmission and reception of radio waves. The radio waves contain information, in the form of a modulation on a carrier wave. This is transmitted from a source to the satellite, which receives that signal and then retransmits it to the intended recipient. For our look at satellite communication, we will start with basic satellite communications architecture. The architecture can be thought of in three segments. These are ground, space, and the communications link between them. The “ground” segment more accurately refers to Earth-based terminals, which could include stationary or mobile terminals traversing land, sea, or air. “Terminal” encompasses the necessary equipment/hardware and software required to transmit to or receive communications.⁷ The communication link portion of the architecture joins the ground and space piece with information transmitted via radio waves, and includes the characteristics of the environment through which it transits (distance, rain, atmosphere, etc.). This link includes communication of both “mission data” (data that serves the purpose the satellite was designed for such as communications

³ Ibid.

⁴ Whalen, “Communications Satellites Short History.”

⁵ Ibid.

⁶ Ibid.

⁷ Wiley J. Larson and James R. Wertz, *Space Mission Analysis and Design*, 3rd. edition (Hawthorne, CA: Microcosm Press, 1999), 534.

or imagery) as well as tracking, telemetry, and command (TT&C) data (for the purpose of controlling and operating the satellite).⁸ The term for information traveling from ground to space is “uplink,” whereas if the direction of travel is from space to ground, the term used is “downlink.” Finally, the space segment consists of the satellite or satellites, designed to receive and transmit information to/from the ground segment via the communication link segment. Depending on the satellite, the transmission to the ground may occur after steps that could include simple amplification, filtering, and translation to a downlink frequency, or more advanced processing to include error correction and signal regeneration.

To understand how these pieces impact communications, the link Equation (1.1) (commonly referred to as link budget) characterizes the strength of the link, typically as the signal-to-noise ratio, based on the factors that affect it. E_b/N_o , the signal-to-noise ratio normalized per bit, directly relates to the probability of bit error through modulation and coding.⁹ On a simpler level, a higher E_b/N_o means fewer errors and better quality. While the link equation can be found in varying forms, one that is useful for a basic understanding is taken from *Space Mission Analysis and Design (SMAD)*.¹⁰

$$E_b/N_o = \frac{PL_t G_t L_s L_a G_r}{k T_s R} \text{ [see footnote]}^{11} \quad (1.1)$$

What helps increase the signal-to-noise ratio is increased transmitter power (P), transmit antenna gain (G_t), receiver antenna gain (G_r), or reduced free space loss (L_s), transmission path loss (L_a), line loss (L_l), data rate (R), and system noise temperature (T_s)¹². The (k) in the equation is Boltzmann’s constant. Not all of these items are adjustable. Free space loss is a function of the distance from the transmitter to the receiver, and therefore is not easily changed when dealing with satellite communications. The Earth’s atmosphere, rain, foliage, and similar obstructions result in transmission path

⁸ Larson and Wertz, *Space Mission Analysis and Design*, 534.

⁹ Ibid., 561.

¹⁰ Ibid., 551.

¹¹ Ibid., 551.

¹² Ibid., 551.

loss, particularly at higher frequencies of communication such as the Ka-band, which is where this thesis will be concerned. Line loss is a function of the hardware used in the ground and space segments of the communication system, and is typically extremely small in comparison to free space loss. The system noise temperature is an equivalent temperature representing the summation of the degrading effect resulting from various sources of environmental noise both natural (e.g., sun or Earth's presence in antenna beam) and man-made (buildings).¹³ Gain for any antenna (transmitter or receiver) is a function of antenna size, wavelength, and efficiency. While the former factors are often difficult to change as characteristics of the environment, transmitter, receiver; transmitter power sometimes can be changed or increased within system constraints to provide an increased E_b/N_o . Data rate may also be decreased to provide increased E_b/N_o and improved communications quality.

B. EMI AND JAMMING OVERVIEW

In satellite communications today a common problem for both civilian and military users is electromagnetic interference (EMI). The *Chairman of the Joint Chiefs of Staff Manual (CJCSM) 3320.02D – Joint Spectrum Interference Resolution (JSIR) Procedures* defines EMI as “any electromagnetic (EM) disturbance that interrupts, obstructs, or otherwise degrades or limits the effective performance of electronics or electrical equipment.”¹⁴ The manual goes on to state that the causes of EMI may be either unintentional or intentional.¹⁵ This should be added to the definition of interference by Carlson and Crilly, which clarifies interference is “contamination by extraneous signals from human sources,”¹⁶ regardless of whether it is intentional or not. Other causes of degradation include noise, which has been defined as “random and unpredictable electrical signals produced by natural processes both internal and external to the system” and distortion, defined as “waveform perturbation caused by imperfect response of the

¹³ Larson and Wertz, *Space Mission Analysis and Design*, 556.

¹⁴ “Joint Spectrum Interference Resolution (JSIR) Procedures,” *Chairman of the Joint Chiefs of Staff Manual (CJCSM 3320.02D)*, June 3, 2013, A-1.

¹⁵ *Ibid.*, A-1.

¹⁶ A. Bruce Carlson and Paul B. Crilly, *Communication Systems: An Introduction to Signals and Noise in Electrical Communications*, 5th edition (New York: McGraw-Hill, 2011), 4.

system to the desired signal itself.”¹⁷ When undesired radio waves/energy are received by the satellite the desired signal and information from the undesired signal and clutter become harder to distinguish. If the undesired and desired signals are unable to be completely and accurately separated from each other, the quality (match of what is received to what was sent) of the transmission is negatively impacted. The scale of the impact depends largely on the relative strength of the various signals involved and the ability of processing, modulations, and coding/error correction methods available to help distinguish desired from undesired signals.

Since out of the three degradation sources (distortion, noise, and interference) interference is the only one caused by humans, that will be our focus—the others can be thought of as the cost of doing business in satellite communications and can also be corrected to some extent. Causes of interference are numerous. Incorrect frequency use by communications users, other transmitters in the antenna beam (ranging from friendly to adversarial), equipment improperly set up or in proximity to other electrical equipment/electronics, or improperly pointed antennas, along with anything else in the form of man-made items or use of them either properly or not. The term jamming in this thesis will be defined as EMI caused intentionally by a hostile emitter.

1. Why EMI/Jamming Is an Issue for the DOD

Satellite communications are extremely important to the Department of Defense. A report by the Government Accountability Office has stated that “DOD’s use of SATCOM is critical to military operations worldwide and its dependency is expected to increase over the next decade.”¹⁸ The same report stated that between 2000 and 2011 the DOD increased commercial SATCOM use by 800%; presumably reflecting close to the total increase in SATCOM use by the DOD due to the small percentage of SATCOM met by DOD-owned assets.¹⁹ The inherent nature of the United States military as a

¹⁷ Carlson and Crilly, *Communication Systems: An Introduction*, 4.

¹⁸ Government Accountability Office. *Defense Satellite Communications: DOD Needs Additional Information to Improve Procurements* (GAO-15-459) (Washington, DC: Government Accountability Office, 2015), 19.

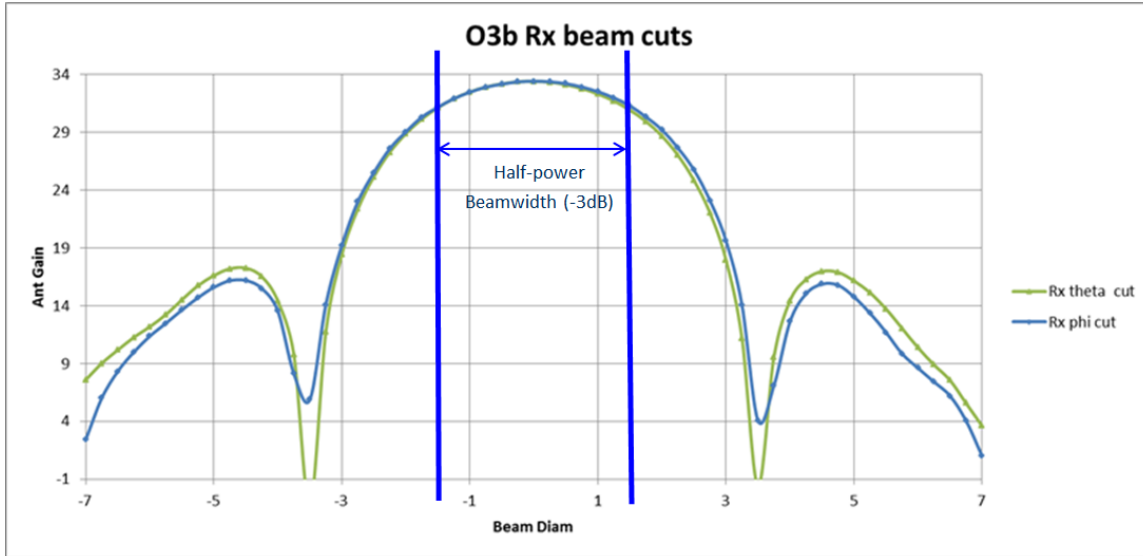
¹⁹ *Ibid.*, 9.

deployable, expeditionary force—expected to execute missions at locations around the globe, often in remote or undeveloped locations—results in a need for a communications structure that can accommodate those missions on minimal notice. Satellite communications contribute to the capability to meet that need. With no permanent ground infrastructure required, small terminals can be deployed and set up or even carried by ship, vehicle, or personnel. These allow command and control, communications, and intelligence to occur unimpeded and be distributed in an expedient manner anywhere in the world. The need for satellite communications capacity has drastically risen with the increased demand for intelligence, surveillance and reconnaissance (ISR) products such as high resolution imagery and video used for battle space awareness and targeting. Any reduction in availability of satellite communications due to jamming could slow or even severely degrade military operations.

2. How Jamming Occurs

In order to understand how jamming typically occurs some geometry must be considered. Before that, antenna gain as it relates to beamwidth must be addressed. Antenna gain at its most basic is a numerical description of the ability to concentrate signal energy that would otherwise be distributed in all directions. For a common parabolic antenna with a circular aperture, an antenna with a larger diameter or operating at high frequencies (shorter wavelengths) is able to concentrate energy better than a smaller one or one operating at lower frequencies (longer wavelengths). The projection of this area of concentrated signal strength onto the Earth (for a satellite-based antenna) can be called the beam coverage area (BCA) or “footprint.” If the antenna in question is located on the Earth and aimed at a satellite, then the BCA would fall in space. The gain is highest in the center of this area (called the boresight) and then falls off in a lobe pattern at increasing distances from center. Due to this pattern, the width of the beam must also specify the level of gain used to characterize that width. The -3 dB point from peak gain is typically used, and the diameter (measured in degrees to accommodate satellite altitudes) is aptly named the “half-power beamwidth.” The beam pattern for an O3b payload antenna demonstrates this concept in Figure 1.

Figure 1. O3b Satellite Payload Antenna Pattern with Half-Power Beamwidth and Side Lobes.²⁰



Moving to the geometry portion of jamming, in order for effective reception of a signal to take place, a transmitter should be located within the BCA at a location with suitable gain to meet the objective. This is true regardless of whether the transmitter is located at the satellite or ground terminal, and regardless of whether the transmitter is the intended one or a hostile emitter—the only difference is that the objective shifts from closing a link to preventing closure of a link if the transmitter is hostile. With SATCOM, the reason the uplink is typically jammed instead of the downlink (a notable exception being GPS jamming, which is not covered in this thesis) is that to jam the uplink the transmitter can be on the earth, and to jam the downlink it would have to be somewhere above the receiver in the beam—such as space.

While satellite communications offer significant advantages over some other forms of communication, they still have vulnerabilities, many resulting from the same things that make them so useful. A fundamental disadvantage of satellite communications is that a critical part, the satellite, has to be in space. This means that it had to be placed in orbit, and that causes constraints on weight, size, and power available. Antenna

²⁰ Adapted from J. J. Shaw, “O3b Networks and Why Not?” (presentation, Naval Postgraduate School, Monterey, May 7, 2015).

diameter (size) is an important factor in the link budget (1.1) that significantly impacts the signal-to-noise ratio. Satellites are also expensive. Furthermore, the purpose of SATCOM as the DOD uses it is often to provide communications to a user who is using a small terminal in order to maintain deployable, expeditionary, and mobile communications. The issue becomes that a jammer on the ground has a dramatic advantage over the satellite when considering cost since there is no cost per pound to lift it to space, and can be comparable to or surpass the friendly force ground transmitter in important aspects affecting gain. The jammer can easily have a large antenna and power supply as even a mobile jammer is only limited by the size and/or number of vehicles required to carry it. A stationary jammer faces even less restriction. While Ka-band technology is more complex than lower frequencies, such as UHF, the technology is widespread and available for purchase in C and Ku bands (an internet search for “Ku-band SATCOM jammer” can demonstrate this) and could reasonably be expected to progress to Ka-band as the band becomes more commonly used, and therefore a larger target.²¹ In countries where Ka-band coverage exists a television news van or other terminal (whether purchased or legally or illegally acquired) set up to transmit by satellite could easily be repurposed as a jammer by the adversary, or inadvertently become one through user error by news crews covering events in the area or due to equipment malfunction.²² Numerous websites show entire fleets of Ka-band operating news vans, many of which are advertised as low-cost.²³

While jamming technology is available and a relatively low cost method of interfering with satellite communications, to be most effective it still needs to be located within the BCA of the satellite’s antenna, and have the transmit antenna oriented at the receiver satellite. Even for Ka-band frequency satellites with relatively small spot beams

²¹ Ronald C. Wilgenbusch and Alan Heisig, “Command and Control Vulnerabilities to Communications Jamming,” *Joint Forces Quarterly*, no. 69 (April 2013): 58.

²² *Ibid.*, 61.

²³ Skylogic. NEWSSPOTTER. (accessed May 17, 2016). http://www.skylogic.it/?page_id=2309&lang=en; C-Com Satellite Systems Inc. Ka-Band. (accessed May 17, 2016). <http://www.c-comsat.com/solutions/ka-band/>; Frontline Communications. Mobile Ka-Band Solution Debuts for Satellite Newsgathering. August 21, 2013. <http://www.frontlinecomm.com/news/KaWriteUp.pdf>.

there can be significant antenna gain over hundreds of km, with an example being O3b, which provides greater than 25 dB gain for an area more than 700 km wide.²⁴ Without publishing where these beams are pointed or unit locations, if hostile forces happen to know where DOD forces are located/operating within hundreds of km, which they likely will if the operations concern them, then they can easily fall within the BCA. Another scenario would be that the actor is detecting down-link signals and could then assume they are within the BCA. Neither scenario is unreasonable. For example, at a 500 km diameter, a beam would cover the majority of Syria. A 1000 km wide beam, on the other hand, would cover nearly all of Iraq. Finding the satellites that are likely used for communications are also relatively simple, as DOD communications satellites such as Wideband Global SATCOM (WGS) are not classified and there is a wide number of amateur astronomy websites available which post ephemeris data for both commercial and military satellites. Furthermore, due to satellite communications being restricted to line of sight and the limited number of Ka-band communications satellites, there would be a small number of options for which satellites could be in use for a given area. This would then allow the hostile force to orient the jammer antenna on the communications satellite to optimize their chances of successful interference.

C. CONCLUSION

With their use on a global scale by the military for important functions, satellite communications are a likely target for adversaries.²⁵ In the past years, intentional jamming incidents have risen rapidly, with numerous incidents of government or political bodies in the Middle East intentionally jamming various satellites having been widely reported.²⁶ One article citing a high-level Eutelsat employee placed the number of intentional interference incidents Eutelsat experienced at 54 in 2010, twice that in 2011,

²⁴ J. J. Shaw, "O3b Networks and Why Not?"

²⁵ Wilgenbusch and Heisig, "Command and Control Vulnerabilities to Communications Jamming," 56–63.

²⁶ *Ibid.*, 58.

and three times the 2011 figure in 11 months of 2012.²⁷ This growing threat of communications jamming is one that will need to be addressed; while geolocation of the jammer does not prevent jamming from occurring, it can help resolve the threat once it occurs.

²⁷ Anne-Wainscott Sargent, "Fighting Satellite Interference on All Fronts," *Via Satellite - SatelliteToday.com*, March 1, 2013, <http://www.satellitetoday.com/publications/via-satellite-magazine/features/2013/03/01/fighting-satellite-interference-on-all-fronts/>.

THIS PAGE INTENTIONALLY LEFT BLANK

II. GEOLOCATION OF EMI SOURCES

Chapter I gave a quick overview of satellite communications, EMI, and why this is a problem for the DOD. Chapter II will first address the importance of the ability to locate the source of EMI. It will next cover some specific characteristics of Ka-band, which are important to the focus of this particular thesis. Finally, it will discuss some existing methods of geolocation and why they are not ideal for use with Ka-band communications.

A. WHY FINDING EMI SOURCES IS IMPORTANT

In *CJCSM 3320.02D*, geolocation/direction finding is listed as a part of the JSIR process following initial detection, verification, characterization, and reporting. Geolocation is important because the resolution process depends on the location, ownership, and users of the problem emitter and the impacted receiver.²⁸ Ownership and users would be difficult to identify without knowing the location of the emitter. Also, although geolocation occurs after characterization in the process, knowing a location could confirm an interference incident was hostile, neutral, or friendly. Finally, even if geolocation fails to provide insight as to the ownership or users of the problem emitter, a location of the emitter can enable mitigation of the interference and restoration of the degraded resource—topics which will be addressed in greater depth later. When dealing with interference incidents outside of simulations such as in this thesis it is important to ensure all information pertaining to the incident and any associated geolocation is classified to the appropriate level—guidance may be found in *CJCSM 3320.02D* Enclosure D.²⁹

B. CURRENT GEOLOCATION TECHNIQUES OVERVIEW

In the search for techniques that could be utilized by O3b communications satellites, the first step was to learn about existing geolocation techniques and evaluate if

²⁸ “Joint Spectrum Interference Resolution (JSIR) Procedures,” A-7–A-13.

²⁹ Ibid., A-6, A-7.

they were suitable for use. Given the variety of methods, these can be organized by similarity in requirements, such as number of satellites/receivers.

1. Multiple Satellite Methods

Two of the most common methods of geolocation are time difference of arrival (TDOA) and frequency difference of arrival (FDOA), which both require multiple satellites. The required geometry for both methods is the same, and consists of two satellites receiving the interference signal simultaneously. With TDOA a specific pulse or portion of the signal must be able to be uniquely identified in order that a time difference in when that pulse is received by the two different satellites may be measured. The time difference then correlates to a difference in distances between the respective satellites and transmitter. A key aspect is that while the difference in distances is known, the magnitudes of each distance is not—as the receiver does not know when the signal was originally transmitted. This difference in time/distances is constant over a number of possible locations which form a line of position (LOP), known as an isochrone, for “same-time.”³⁰ A single line of position is inadequate for a geolocation, but when various TDOAs are collected or another method is used to obtain an LOP then positional ambiguity can be resolved and accuracy is increased. This method is well discussed in Dr. Herschel Loomis’ paper *Geolocation of Electromagnetic Emitters*.³¹ The paper also discusses a similar TDOA approach, the “Interferometric Approach,” in which if the distance between satellites is small compared to the distance to the transmitter, the math may be simplified and results in an angle giving the isochrone/LOP.³² The resultant line is noted to be the “same line which defined the asymptotes of the hyperbolic isochrones.”³³ An example of TDOA isochrones from *Geolocation of Electromagnetic*

³⁰ Herschel H. Loomis, *Geolocation of Electromagnetic Emitters* (NPS-EC-00-003), (Monterey: Naval Postgraduate School, Revised October 2007), 1.

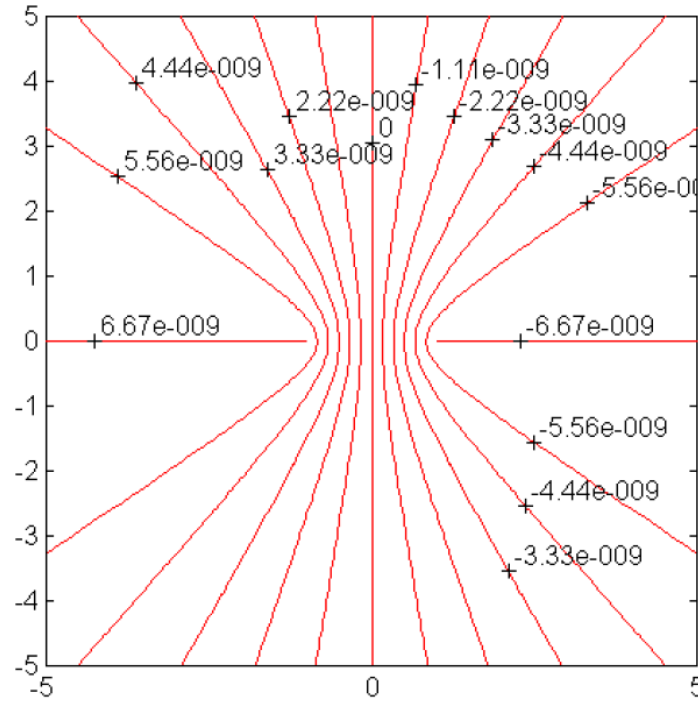
³¹ Ibid.

³² Ibid., 6.

³³ Ibid., 5–6.

Emitters is shown in Figure 2, where the satellite would be moving left to right along the x-axis.³⁴

Figure 2. Family of Hyperbolic TDOA Isochrons.³⁵



FDOA is often used as the complement to the TDOA LOP. The reason that these methods work well together is that while TDOA provides an LOP that is generally an angle along which the emitter lies, FDOA provides a range.³⁶ The FDOA/range LOP intersects the TDOA LOP to provide a geolocation. FDOA once again requires two satellites that receive the signal from the transmitter simultaneously. FDOA also requires that the satellites are moving at sufficient speed to generate a Doppler shift significant in comparison to the ability to measure frequency (so it is not lost in measurement error). Doppler shift (Δf , Hz) as shown in Equation (1.2) is a result of the velocity (v , in m/s)

³⁴ Loomis, *Geolocation of Electromagnetic Emitters*, 5.

³⁵ Source: Loomis, *Geolocation of Electromagnetic Emitters*, 5.

³⁶ Darko Musicki and Wolfgang Koch. "Geolocation using TDOA and FDOA Measurements," in *Proceedings of the 11th International Conference on Information Fusion*, (Cologne: IEEE, 2008), 1987–1994.

component of the receiver along vector r connecting the transmitter and receiver. This is then multiplied by the frequency (Hz) and divided by the speed of light (c , m/s). Convention is that if the range from receiver to transmitter is decreasing v and Δf are positive.

$$\Delta f = \frac{f}{c} \frac{v \cdot r}{|r|} = \frac{f}{c} v \cdot \hat{r} = \frac{f}{c} v_{rel} \quad (1.2)$$

This is because if the transmitter and receiver are closing in distance then signal waves are compressed which results in a frequency upshift. If the transmitter and receiver are increasing in respective range then frequency downshift occurs as the signal waves are spread more. If there was no relative motion the Doppler shift would be 0. The FDOA Equation (1.3), as taken from *Geolocation of Electromagnetic Emitters*, for frequencies f_1 and f_2 received by receivers 1 and 2, respectively, demonstrates in two dimensions how the known receiver velocities and measured FDOA would relate to a LOP characterized by x and y coordinates.³⁷ This equation represents a situation where the receivers are located on the x -axis at $(s, 0)$ and $(-s, 0)$, each moving at velocity (v_x, v_y) , and the emitter is at (x_e, y_e) .³⁸

$$\text{FDOA} = f_2 - f_1 = \frac{f}{c} \left(\frac{v_x(x_e + s) + v_y y_e}{\sqrt{(x_e + s)^2 + y_e^2}} - \frac{v_x(x_e - s) + v_y y_e}{\sqrt{(x_e - s)^2 + y_e^2}} \right) \text{ [see footnote]}^{39} \quad (1.3)$$

This equation is the result of taking the difference of the Doppler shift received by each receiver (as seen in Equation (1.2) for a single receiver), and then expanding the velocity of the receivers and r vectors between each receiver and emitter into components. The solution to Equation (1.3) results in an LOP giving range. When used in conjunction with TDOA giving bearing, or other LOPs the ambiguity is resolved and results in a geolocation. This is demonstrated in Figure 3 taken from *Geolocation of*

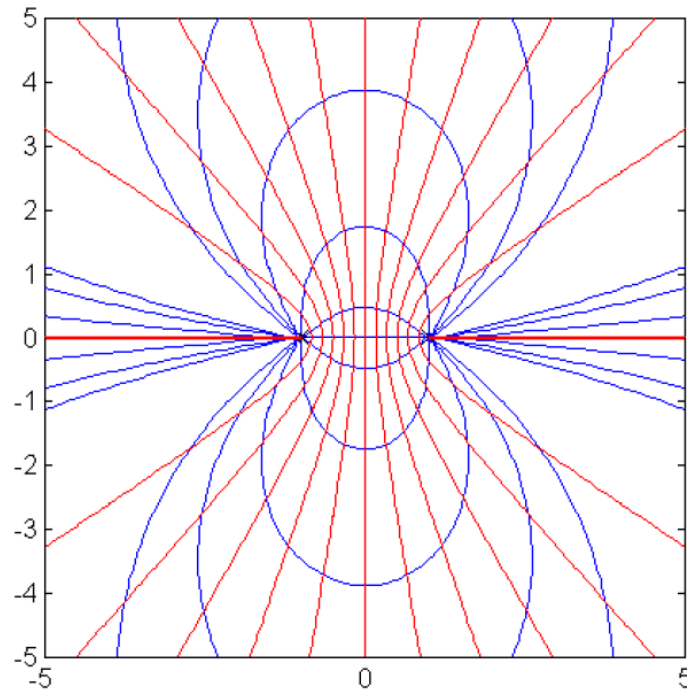
³⁷ Loomis, *Geolocation of Electromagnetic Emitter*, 6–7.

³⁸ Ibid., 7.

³⁹ Ibid., 7.

Electromagnetic Emitters, which shows how FDOA contours (blue) complement the TDOA isochrones (red) to create intersections that would identify a position.⁴⁰

Figure 3. TDOA and FDOA Contours.⁴¹



2. Multiple Antenna Methods

For methods of geolocation using multiple antennas a common method is angle of arrival (AoA), basically using the interferometric approach to TDOA as discussed previously, but with the receivers as multiple antennas on a single satellite as opposed to on multiple satellites. An alternative method which has been modeled and may currently be undergoing real world testing is using steerable beams to create a pattern of footprints from which signal strength differences created by the emitter's varying location in each beam can be used to calculate lines of position.⁴²

⁴⁰ Loomis, *Geolocation of Electromagnetic Emitters*, 10.

⁴¹ Source: Loomis, *Geolocation of Electromagnetic Emitters*, 10.

⁴² Brian C. Fredrick, "Geolocation of Source Interference From A Single Satellite With Multiple Antennas" (master's thesis, Naval Postgraduate School, 2014).

3. Single Antenna Methods

The primary method of using a single antenna for geolocation of an emitter is interferometry. This method is analogous to TDOA/AoA, as phase difference is directly related to time difference. The difference is simply in what property is able to be measured based on the situation. For single-antenna interferometry typically a phased array antenna is used which has elements spaced extremely close together, at less than half the wavelength of the transmitted frequency. The spacing is important as there would otherwise be ambiguity as to whether the measured phase difference was correct or off by a multiple of 2π . By measurement of the phase difference in the signal as received by two elements on the array, and using the known wavelength, an angle may be computed. A phase difference that correlates to the spacing between elements would mean that the two elements formed a line pointing towards the transmitter, whereas no phase difference would mean that the elements lie on a line perpendicular to a line to the transmitter (a bearing line). Of course, in between these boundary scenarios lie phase differences correlating to a number of other transmitter bearings. The bearing line calculated, as with the interferometric approach to TDOA, is the asymptote of a hyperbola with the foci at one of the receiver elements. Which asymptote the transmitter lies on is initially ambiguous as the sign of the angle calculated is unknown, until the method is repeated with other elements. This method and the associated math developing the asymptote lines for the hyperbolas are detailed in *Radio Interferometric Angle of Arrival Estimation*.⁴³

An alternative method of geolocation using a single antenna is through the use of the Doppler effect. The significant advantage of the use of the Doppler effect is that it requires only a single antenna on a single satellite, and does not require *a priori* transmitter frequency knowledge. The Doppler effect varies in accordance with relative velocity of the transmitter to receiver, as Equation (1.2) previously showed. The relative velocity, when the transmitter is stationary and the orbit is known, can be correlated to physical location.

⁴³ Isaac Amundson et al., “Radio Interferometric Angle of Arrival Estimation,” in *Proceedings of 2010 European Conference on Wireless Sensor Networks*, (Coimbra: Springer, 2010).

C. WHY GEOLOCATING EMI SOURCES IN KA-BAND IS CHALLENGING

The military today requires high quantities of data to accommodate everything from everyday communications for operations, to morale boosting applications, to large quantities of intelligence. The required bandwidth is only increasing, as discussed in Chapter I, Section B.1. Other frequency bands, such as C and Ku-band generally support lower data rates, have wider beam coverage areas, many more users, all resulting in them becoming increasingly congested. This is going to result in the military increasingly shifting to Ka-band to facilitate its needs, and with the increased shift to Ka-band will come the need for geolocation services in the Ka-band.

There are numerous challenges to geolocating Ka-band EMI sources. Many of the same characteristics that make Ka-band satellites' use beneficial, such as their difficulty to jam when compared with lower frequencies, also make using them for geolocation challenging. Military Ka-band operates with typical uplink frequencies of about 30 GHz, as seen in the WGS constellation.⁴⁴ Commercial Ka-band is close to that, though typically slightly lower. Use of higher frequencies provides increased bandwidth which can support either higher levels of protection through frequency spreading or hopping, or support much higher data rates than lower frequencies. These characteristics and others related to them are useful in making communications more robust, but these frequencies and the current constellations also eliminate several existing techniques as options for geolocation of EMI sources.

1. Number of Satellites

Currently, there are significantly fewer satellites operating in Ka-band than in other frequencies such as C or Ku-band. While this helps with congestion and reduces the likelihood of unintentional interference, there are types of geolocation methods such as FDOA and TDOA which utilize multiple satellites. For these methods, each satellite must have the jammer within the antenna's footprint to compare information about the signal as it is received by other satellites at the same time. To remedy this problem, a method

⁴⁴ Richard A. William, and Heywood I. Paul, "Potential Uses of the Military Ka-band for Wideband MILSATCOM Systems," in *Military Communications Conference*, (Boston: IEEE, 1998), 30–34.

able to provide Ka-band frequency geolocation using a single satellite and single antenna on that satellite should be used if possible.

2. Antenna Gain and Beamwidth

The higher frequencies that fall under Ka-band give greater antenna gains at smaller sizes, making Ka-band more suitable for mobile/on-the-move systems requiring high data rates than lower frequencies. The antenna gain Equation (1.4) taken from (*SMAD*) is shown below, where D is antenna diameter in meters, η is an efficiency factor, and λ is wavelength in meters.⁴⁵

$$G = \frac{\pi^2 D^2 \eta}{\lambda^2} \quad [\text{see footnote}]^{46} \quad (1.4)$$

A quick comparison of the 30 GHz Ka-band uplink to a 12 GHz Ku-band signal with a 1 meter antenna (for ease of math) using the above equations shows the Ka-band signal has a gain of more than six times (about 8 dB) greater than at the Ku-band frequency. This larger gain can help overcome interference or otherwise improve the link budget to better meet the needs of the user.

The higher frequency of Ka-band also gives a smaller beamwidth for a given antenna size. The half-power (defined as a 3 dB drop in signal strength from beam center) beamwidth Equation (1.5) as taken from *SMAD* is shown, where beamwidth is in degrees, D is antenna diameter in meters, and f_{GHz} is the frequency in GHz.⁴⁷

$$\theta = \frac{21}{f_{GHz} D} \quad [\text{see footnote}]^{48} \quad (1.5)$$

Another quick comparison of a 30 GHz signal for a Ka-band uplink to a 12 GHz Ku-band signal with a 1 meter antenna shows the Ka-band signal has a half-power

⁴⁵ Larson and Wertz, *Space Mission Analysis and Design*, 553.

⁴⁶ Ibid.

⁴⁷ Ibid., 555.

⁴⁸ Ibid.

beamwidth of .7 degrees, where the Ku-band frequency has a half-power beamwidth of 1.75 degrees. The difference may seem insignificant, but at GEO one degree difference is over 600 km. If the Ka-band system is at MEO instead, the difference may be almost 1000 km. The wider beams that are resultant from lower frequencies (such as Ku-band) mean that a ground-based emitter's beam is more likely to encounter multiple GEO slots/satellites, and satellites near each other in GEO are more likely to have overlapping BCAs on the ground. Due to these conditions, the probability of multiple satellites receiving interference from a common transmitter is higher, and with that, the ability to conduct multiple satellite geolocation techniques is also more likely. The same conditions and opportunities are unlikely for a Ka-band system due to the much smaller beamwidths and possibility of multiple satellites receiving interference from a common transmitter.

A common term used to describe the small and typically steerable beams now frequently used by Ka-band and high throughput satellites (HTS) is “spot beam,” which is in contrast to very wide beams designed to cover a larger area of the Earth (sometimes everything in the line of sight) without steering. This smaller beam is a desired and purposefully engineered aspect of Ka-band satellites, as it provides numerous benefits. A small, steerable beam is able to concentrate gain where it is most needed (or paid for) while wasting less on areas that the user does not serve. The spot beam also makes jamming more difficult due to the fact that the emitter must be within a smaller geographic area to fall within the BCA. This could mean within a 1000 km radius instead of on the correct one-third of the world for an Earth Coverage (EC) antenna, example.

Spot beams also allow for frequency reuse, which allows spectrum to be separated geographically. This helps prevent unintentional interference from neighboring beams and also allows the finite and allocated spectrum to be used several times, supporting more users (and profit, in the commercial sector). High throughput satellites such as INMARSAT Global Xpress and ViaSat use multiple feeds for each reflector to create patterns of spot beams to allow for frequency reuse. O3b accomplishes this differently, taking advantage of the smaller antenna sizes at Ka-band to support frequency reuse by allowing for many steerable antennas to be placed on moderately sized satellites.

All of these characteristics help make Ka-band a desired frequency range for use, but not for support of TDOA/FDOA geolocation. TDOA/FDOA, requiring multiple satellites, would be highly unlikely to have spot beams placed in the same location, as one of the benefits is that they can be moved to support dispersed or entirely different users. Narrow beams at Ka-band from the jammer uplink would also not be able to simultaneously target multiple satellites, making TDOA/FDOA further unlikely. If multiple beams from the satellite could be steered to cover the same area to perform the geolocation that would remove those beams from their primary mission of communication until the geolocation has been performed. This would interrupt service across a wider area than was originally impacted. For example, every time a jammer degraded communications for one beam, the operator would then interrupt communications on other beams to find it. If an adversary realized that was the technique, it could easily encourage instead of discourage jamming. This also presumes that the user experiencing interference operates the other beams and thus moving them is even a choice (albeit a poor one). Leasing a second or third beam only for geolocation purposes is far from ideal. This same reasoning is applied to why single satellite/multiple antenna geolocation methods are not ideal for use, particularly as it pertains to a non-GEO communications constellation (such as O3b for the focus of this thesis). With moving satellites multiple beams would need to be leased on each satellite, otherwise the ability to perform geolocation would be dependent on which satellite was overhead at the moment. Once again, an ideal geolocation method could use a single spot beam on a single satellite in order to minimize disruption and maximize efficient use of resources.

Single antenna methods of geolocation appear ideal for use by O3b Networks to support interference geolocation for military customers. O3b, however, does not use phased array antennas that are capable of measuring phase difference or performing interferometry. With the only other single antenna method being use of the Doppler effect, it appears a potentially viable method for use that requires substantially fewer resources than other common methods. This will be addressed in greater depth in Chapter III.

D. CONCLUSION

In this chapter, it was established that geolocation of EMI emitters is an important piece of the JSIR process. It was also established that Ka-band geolocation methods must overcome challenges such as relatively few satellites and relatively small antenna footprints. These make methods of geolocation such as TDOA and FDOA unsuitable. Using a single antenna method of geolocation would conserve assets, and use of Doppler shift could be a way to effectively execute it.

THIS PAGE INTENTIONALLY LEFT BLANK

III. O3B AND SUITABILITY FOR GEOLOCATION TECHNIQUE(S)

O3b is a satellite communications company that provides high-data-rate communications to customers through steerable spot beams. O3b has completed various testing objectives with the U.S. military, among those a test with 7th Fleet during Trident Warrior 2015, work with the Marine Corps Tactical Systems Support Activity (MCTSSA), and demonstrations with the Space and Naval Warfare Systems Command (SPAWAR) Common Optical Distribution Architecture (CODA) lab.⁴⁹

A. CONSTELLATION DESIGN

The O3b constellation uses a circular orbit ($<.001$ eccentricity), currently in one equatorial (incline of about $.05^\circ$ or less) plane. The orbit is at an altitude of approximately 8062 km, which is a relatively low (compared to Global Positioning System/GPS satellites) MEO orbit, with an orbital period of approximately 4.8 hours.⁵⁰ The constellation currently contains 12 satellites.⁵¹ At least six satellites are required to provide continuous service as designed (with specified overlap/make-before-break hand-off).⁵² There are also plans to expand service by increasing the number of satellites in the current plane, and there has been some hypothetical discussion about eventually adding two inclined planes that would provide polar coverage.⁵³

B. SATELLITE CHARACTERISTICS

O3b satellites have 10 steerable customer antennas and two steerable gateway antennas.⁵⁴ The antennas are maneuverable to provide what O3b calls “optimal

⁴⁹ O3b Networks, “O3b Government USG Bulletin,” O3bNetworks.com, July 16, 2015, http://www.o3bnetworks.com/wp-content/uploads/2015/08/USG-Bulletin_16JUL15.pdf.

⁵⁰ Steven H. Blumenthal, “Medium Earth Orbit Ka Band Satellite Communications System,” in *MILCOM 2013 - 2013 IEEE Military Communications Conference*, (San Diego: IEEE, 2013), 273–277.

⁵¹ J. J. Shaw, “O3b Networks and Why Not?” (see chap. 1, n. 20).

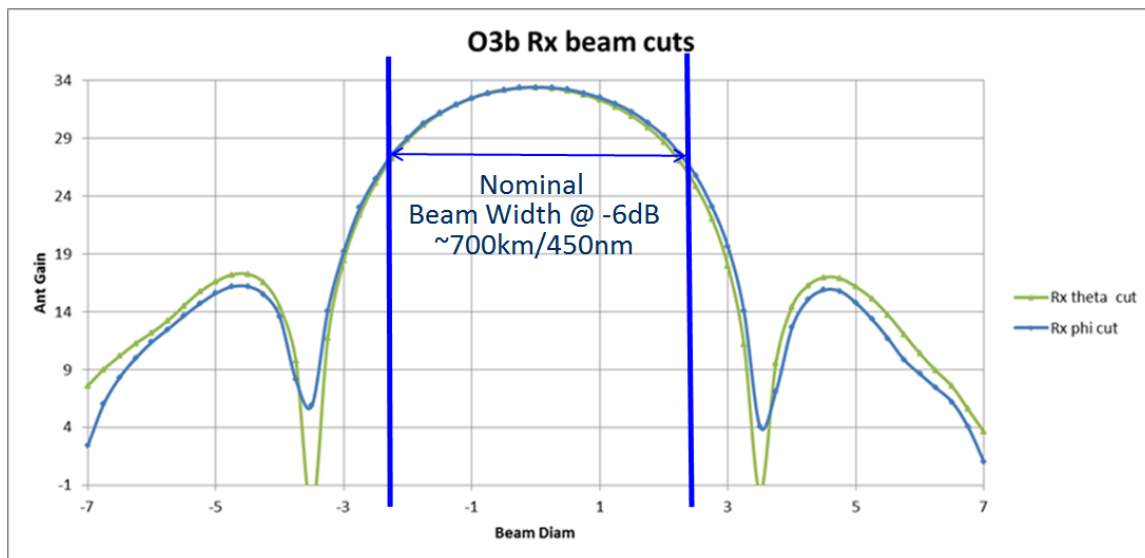
⁵² Ibid.

⁵³ Ibid.

⁵⁴ Ibid.

coverage” to latitudes up to 45 degrees North or South, and “extended coverage” from 45–62 degrees North or South.⁵⁵ Each antenna is parabolic with a circular aperture, the diameter is approximately .4 m.⁵⁶ Satellites currently operate in commercial Ka-band, which uses 27–29 GHz uplink frequencies and downlink frequencies of about 17–19 GHz.⁵⁷ O3b generally considers the widest beamwidth for communications, “outer coverage,” to be five degrees (2.5 degrees off boresight), which is the -6 dB gain point, as can be seen in Figure 4.⁵⁸ This is approximately 700 km in width at nadir, as shown in Figure 5.⁵⁹

Figure 4. O3b Satellite Payload Antenna Receive Pattern.⁶⁰



⁵⁵ J. J. Shaw, “O3b Networks and Why Not?”

⁵⁶ Ibid; Ken Mentasti, email message to author, November 11, 2015.

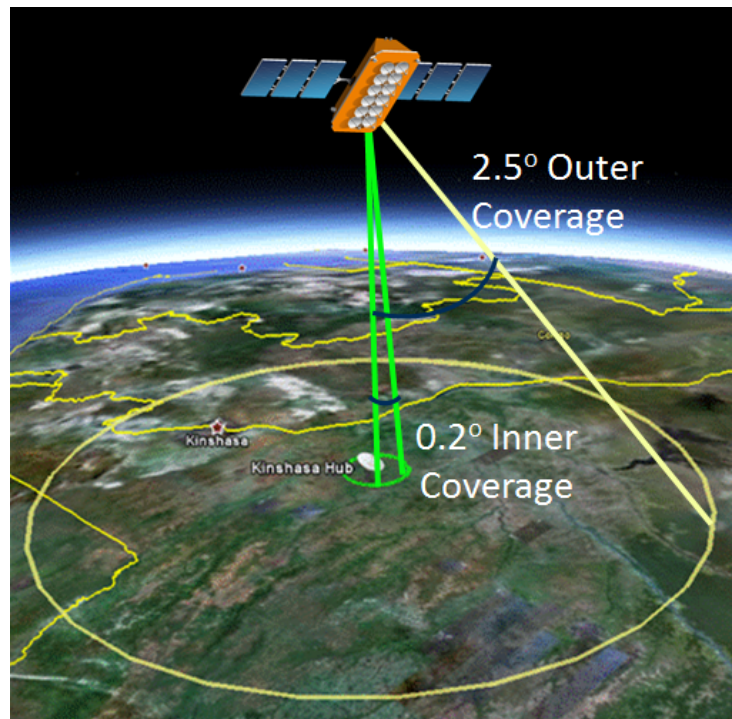
⁵⁷ J. J. Shaw, “O3b Networks and Why Not?”

⁵⁸ Ibid.

⁵⁹ Ibid.

⁶⁰ Source: J. J. Shaw, “O3b Networks and Why Not?”

Figure 5. O3b Beam Coverage.⁶¹



C. USEFUL CHARACTERISTICS FOR GEOLOCATION

As was covered in Chapter II, a method of geolocation of EMI sources using a single antenna would be ideal as it would minimize the impact on valuable communication resources. Without a phased-array antenna enabling the performance of single-antenna interferometry, the single antenna method that remains is use of the Doppler effect, although the exact application is only determined through the rest of this thesis. O3b, located in a MEO orbit, has a greater relative velocity to a stationary transmitter as compared to a communications satellite in a GEO orbit. The high frequencies of Ka-band matched with the greater relative velocities also contribute to a large Doppler shift—as could easily be seen from Equation (1.2), compared to other typical frequency/orbit combinations. To give an idea of the magnitude of the velocity difference, an O3b satellite is traveling more than 5.25 km/s, whereas a GEO satellite is traveling at approximately 3.07 km/s. That is a difference of more than two km/s, or

⁶¹ Source: J. J. Shaw, “O3b Networks and Why Not?”

about 4877 miles per hour. This is not an insignificant amount, and as a result the Doppler shift is much larger, easier to measure, and use.

The relative motion created by the MEO orbit of O3b and the ability to steer beams is also important for use with a method that would employ Doppler shift measurement. A significant reason is that if there is an instant, at which the closing velocity between the EMI source and satellite is zero, then the Doppler shift would also be zero, and the frequency received would match the base frequency of the EMI source. This will occur when the interference source passes abeam the satellite's position within the beam coverage area. With a steerable beam, the beam can be placed along a line perpendicular to the satellite's ground track (abeam), at the satellite's position to ensure this occurs. For a satellite with no inclination this would mean the same meridian as the satellite was positioned over. This is also made possible by the fact that the satellite, at MEO, will assuredly pass the abeam point due to its speed at faster than the Earth's rotation. With communications satellites at GEO, motion relative to the Earth is extremely limited by comparison to O3b and in many circumstances the emitter would never pass into the abeam position. This is a key factor in using Doppler for geolocation, because the exact frequency of an interference source could easily be unknown. Without knowing what base frequency is added to the Doppler shift (Δf) to create the frequency actually received/measured at the satellite, there is no way to determine the Doppler shift present at the varying times throughout the interference event. While the moment the interference source passes abeam would have to be identified somehow, doing so would provide an LOP perpendicular to the satellite's motion as well as identify the base frequency. Without the motion due to O3b's unique orbit ensuring the emitter passes abeam, this LOP would not be possible. With the base frequency established all other received frequency data could now be used for the Doppler shift it contains in order to correlate a position.

The steerable beams of O3b satellites also enable the extended coverage area of up to 62 degrees North or South, potentially providing geolocation services over that entire range. A constellation of 12 satellites, each with an orbital period of 4.8 hours, further means that a satellite is passing every location within the covered latitudes dozens

of times each day (four times per satellite). This would provide multiple opportunities for an EMI source to be located.

D. CONCLUSION

The O3b constellation may provide a useful opportunity for a commercially provided geolocation service. O3b's satellites and constellation differ significantly from most communications satellites on orbit today by use of a medium Earth orbit. The velocity of the satellites relative to Earth and Ka-band frequencies serve to increase the Doppler shift that would be received. The number of satellites, revisit time, and steerable beams all work to increase the number of opportunities and the responsiveness of any potential geolocation. These characteristics all favorably support the potential ability of O3b to be used for a Doppler-based geolocation technique.

THIS PAGE INTENTIONALLY LEFT BLANK

IV. GEOLOCATION TECHNIQUE

Chapter III established that O3b has unique characteristics that make possible a new method of geolocation using the received frequency from an emitter over time. While the characteristics of Doppler and O3b's orbit make a longitudinal LOP seem readily accessible, the specifics of that technique still need to be addressed, as does a way to create an intersecting LOP. To do this, this chapter will start by looking at another application of Doppler shift, and then adapt it to a simplified geolocation problem. Once this has been completed, the method for modeling a more complex situation will be introduced. This model was then used throughout the final section, which addresses added complexity and realism.

Geolocation of an EMI source has the potential to be a complicated problem when attempting to consider every possible situation that could occur in the real world. These situations could include moving emitters at speeds ranging from those of aircraft to those of boats or man, various altitudes due to terrain or aircraft, or transmitters that vary in frequency, among many more. While some of these more complicated situations have been addressed in at least a few other sources,⁶² this thesis was not intended to solve those issues but rather develop and provide proof of concept for a method that could be readily applied to the O3b Network satellites with some utility for DOD operations. To accomplish that, emitters were assumed to be: stationary, fixed transmit frequency, continuously emitting, and located on the surface of a rotating Earth as represented by an ellipsoid. Furthermore, the O3b satellite orbits were simplified to be perfectly circular (zero ellipticity) and equatorial (zero inclination). Also, intentionally left out is the small effect the time for the signal to travel from the emitter to satellite would have on accuracy, as the technique lacks the precision to make that important.

⁶² Tina L. Chow, "Passive Emitter Location Using Digital Terrain Data" (master's thesis, Binghamton University of State University of New York, 2001); Hanna Witzgall, "A Reliable Doppler-Based Solution for Single Sensor Geolocation," (paper presented at the IEEE Aerospace Conference, Big Sky, March 2013).

A. TECHNIQUE DEVELOPMENT

Use of Doppler shift to locate or refine the location of objects by aircraft/satellite is not new. An application used commonly for many years now in both military and civilian applications is Doppler beam sharpening of radar returns, such as with synthetic aperture radar.⁶³ All that is necessary then to use Doppler for geolocation of EMI sources instead of terrain is to make the geolocation situation similar to Doppler beam sharpening. The method often used for Doppler beam sharpening contains both some differences from and similarities to what would need to be done in the circumstances of O3b locating an EMI emitter. In the use of Doppler beam sharpening the frequency is known. This is a significant advantage over locating an emitter with unknown frequency as the Doppler shift can be calculated directly and immediately from the received frequency. The Doppler shift correlates to an isodop, which is a hyperbola shaped LOP, anywhere along which if a transmitter (or reflector) was positioned would cause the same Doppler shift to occur.⁶⁴ Doppler beam sharpening also uses a pulse emitted by the satellite that will later be received (by the satellite), allowing for calculation of the range from the amount of time it takes the signal to return.⁶⁵ This is also a significant advantage as it provides the second necessary LOP (a circular one) necessary to limit the possible geolocation to four points.⁶⁶ Half of those are eliminated by the known factor of which side the radar was observing, and one of the remaining two points is eliminated by whether the Doppler shift was positive or negative (indicating whether the emitter lies on the symmetrical isodops either ahead or behind the satellite's position).⁶⁷ The technique used to eliminate positional ambiguity to the left or right of the satellite's path is easily adapted to O3b as the beam receiving interference can be steered to and then known to be located on one side or the other.

⁶³ John C. Curlander and Robert N. McDonough, *Synthetic Aperture Radar Systems and Signal Processing* (New York: John Wiley & Sons, 1991), 17–26.

⁶⁴ *Ibid.*, 18–19.

⁶⁵ *Ibid.*, 18–19.

⁶⁶ *Ibid.*, 18–19.

⁶⁷ *Ibid.*, 18–19.

The differences highlighted between a Doppler beam sharpening application and a geolocation of EMI sources clarify the issues that need to be resolved in order to use Doppler shift to create a geolocation. The first is that the transmitted frequency needs to be identified because the source is not the satellite, as it is in Doppler beam sharpening. The next issue is how to obtain a range LOP from Doppler when, once again, the source of the transmission is not the satellite and therefore the origination time and transit time are unknown. Resolving the first issue would yield an LOP identifying the EMI source as abeam, thereafter requiring an LOP giving range or cross-track distance (the second issue) from the satellite in order to locate the EMI source.

To evaluate the existing issues, it is useful initially to simplify the problem to a flat, non-rotating Earth and observe data that would be generated and usable for the geolocation process, and how that data appears to vary with location. A dataset for a real world situation could contain the received frequency (base frequency plus Doppler shift), which is easily monitored, and the timestamp for each of those data points. A satellite position at each of those times could also be easily obtained through use of GPS in the case of O3b, or ephemeris data if necessary, both of which can have very good accuracy.⁶⁸ To best relate the data received to a transmitter location, MATLAB⁶⁹ was used to both generate and plot Doppler shift curves with varied but known transmitter location paths (due to the relative motion of satellite/transmitter) and a known transmit (base) frequency. Once the relationship between the Doppler shift over time, base frequency, and transmitter location over time are characterized, then the base frequency and location can become variables which are solved for by analysis of the received frequency over time.

Consider the situation shown in Figure 6. The range, R , is a function of X , Y , and Z , where X is the in-track range, Y is the cross-track range, and Z is the satellite altitude. The in-track range varies over time due to the velocity of the satellite over Earth, v_{sat} , and the starting in-track range, for time at zero seconds, is C . The dotted red lines in the

⁶⁸ Ken Mentasti, email message to author, November 11, 2015.

⁶⁹ MATLAB is a registered trademark of MathWorks.

figure are intended to show the change over time from the initial position. The range between the satellite and EMI source at any point in time is given by Equation (1.5).

$$R = \sqrt{\left((C - v_{sat}t)^2 + Y^2 + Z^2\right)} \quad (1.5)$$

From this equation, the first derivative can then be easily found to give the relative velocity necessary for the Doppler shift equation, Equation (1.2). When added to the base frequency, this results in the frequency that would actually be received by a satellite.

Figure 6. Flat Non-rotating Earth Geolocation Geometry.

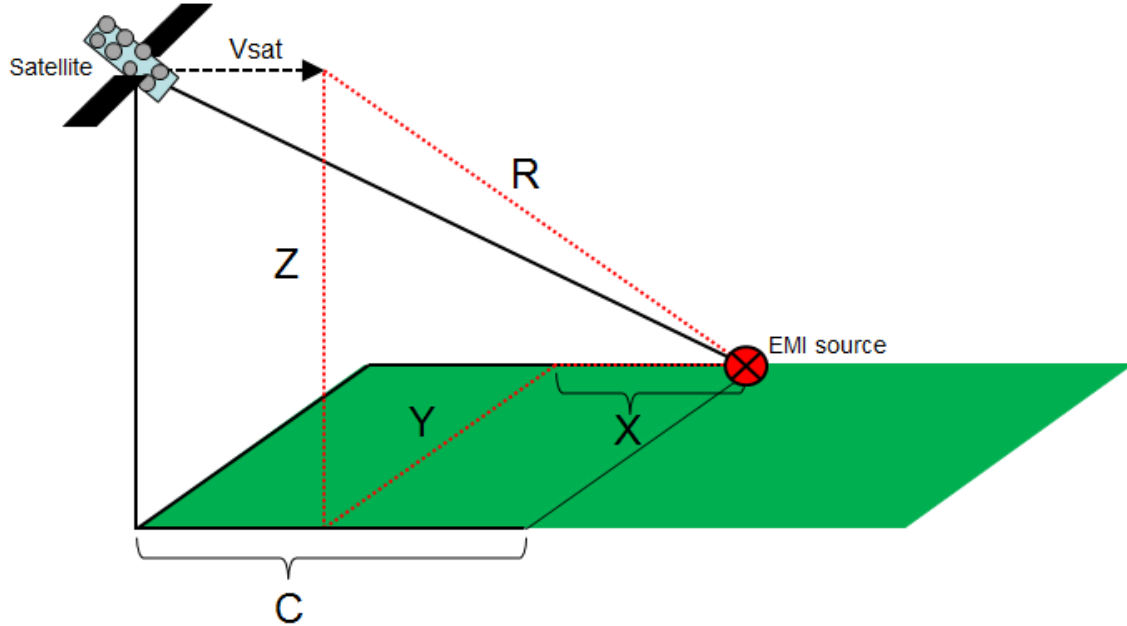
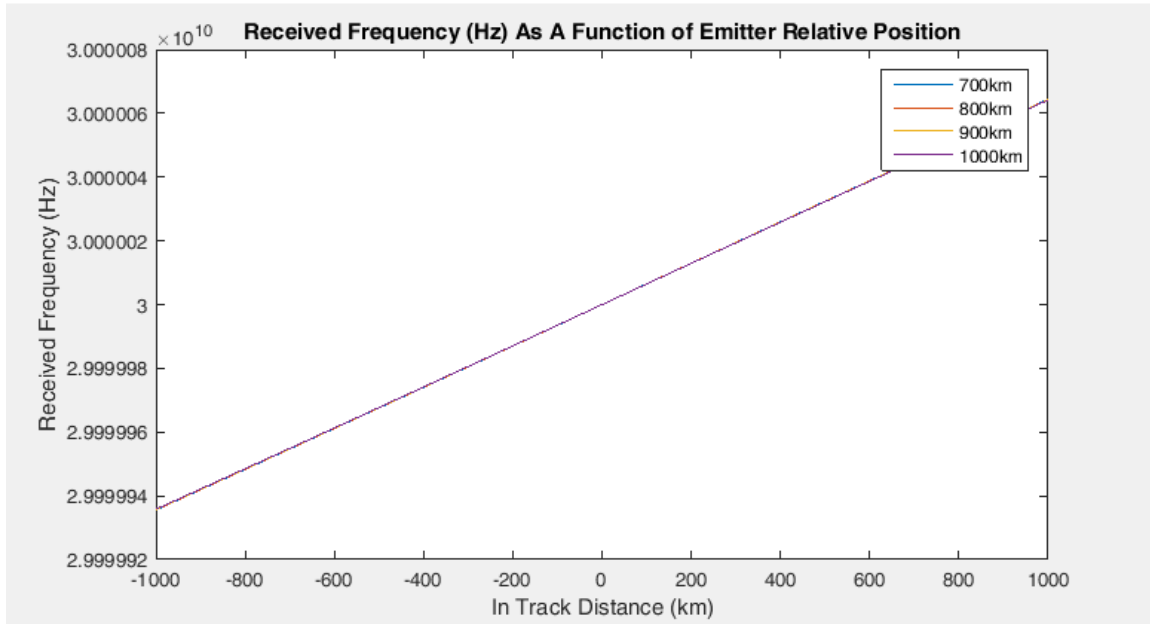


Figure 7 was created in MATLAB. The figure shows the frequency that would be received (Y-axis of Figure 7) by an O3b satellite traveling at orbital velocity over a flat, non-rotating Earth, for various in-track distances (X-axis, positive is ahead of satellite) and cross-track distances (each of four lines plotted, better resolution in Figures 7–9) of an emitter with a base frequency of 30 GHz. When related to Figure 6, Figure 7 represents a situation where in-track distance is based on Vsat=5.255 km/s and C=1000

km. Z would be an altitude of 8062 km and each curve in Figure 7 would represent a different Y, 700 km, 800 km, 900 km, and 1000 km.

Figure 7. Received Frequency as a Function of Emitter Relative Position.



While Figure 7 gives some perspective, it is not precise enough to be useful. For that, closer observation is needed at three general areas of concern: prior-to-abeam, abeam, post-abeam. Figure 8 is a higher resolution graph for when the four emitters are approximately 1000 km ahead of the receiving satellite (and closing) at their respective cross track distances (given in the legend). Figure 9 is a higher resolution graph as the emitters transit the abeam location at their respective cross track distances, from .5 km ahead of to .5 km behind the satellite. In Figure 9 the curves intersect at $x=0$ (abeam) and are indistinguishable from each other at the scale given. Figure 10 portrays the received frequency as the emitters are approximately 1000 km behind the satellite (and getting farther).

Figure 8. Doppler Shift from Emitters Located ahead of Satellite.

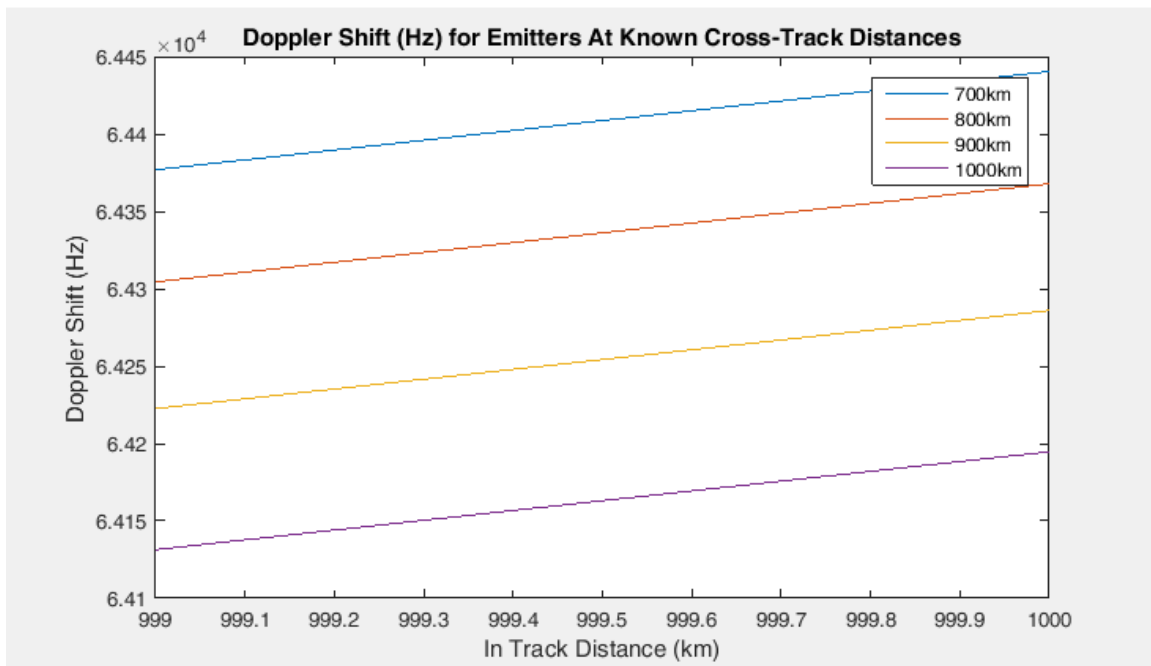


Figure 9. Doppler Shift from Emitters Transiting abeam Satellite.

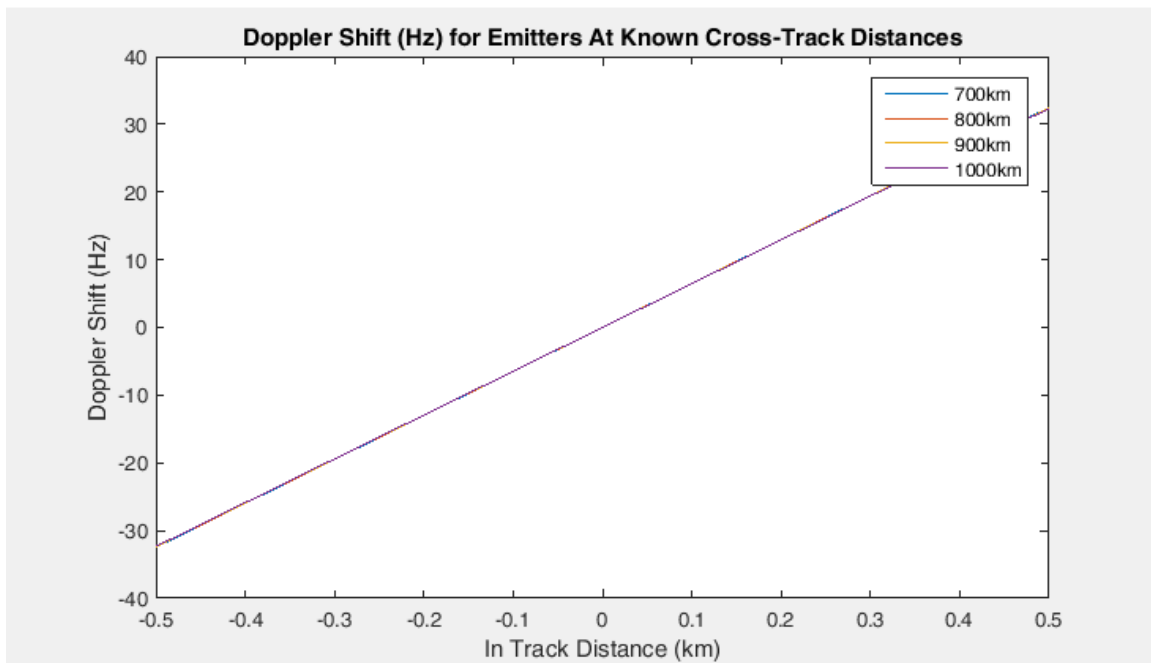
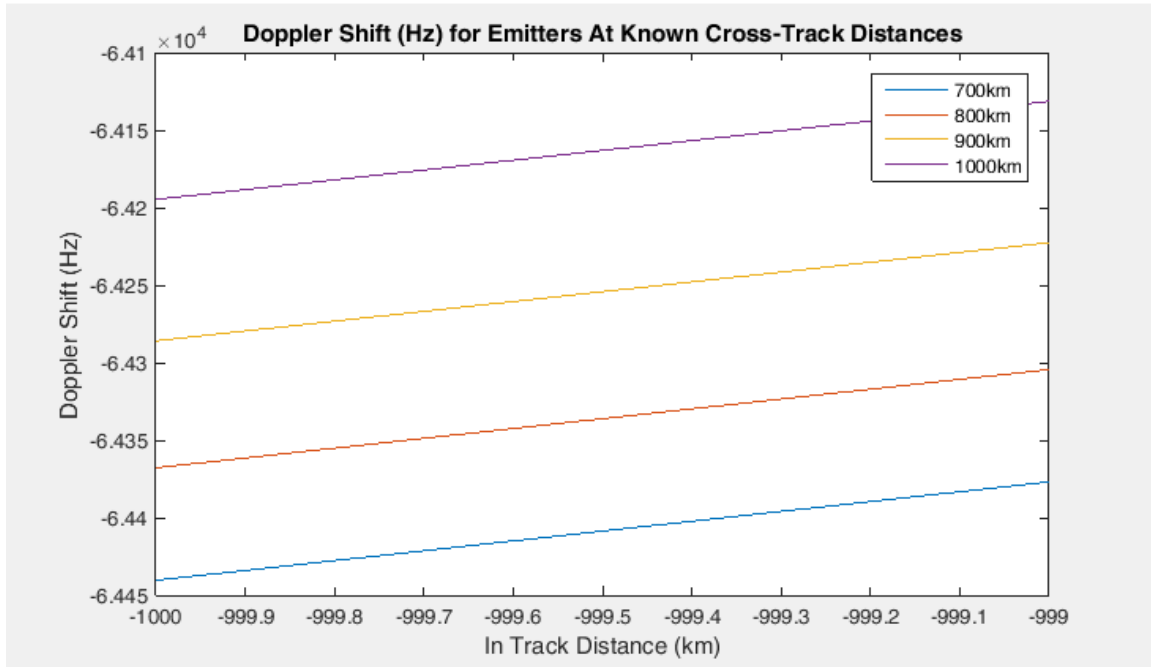


Figure 10. Doppler Shift from Emitters Located behind Satellite.



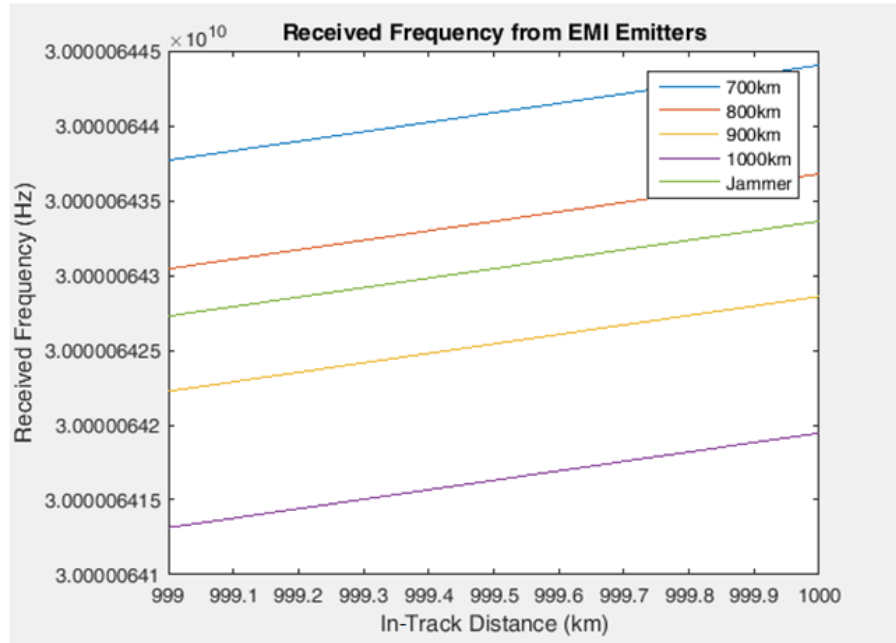
In Figures 8–10 several useful pieces of information can be readily observed that demonstrate analysis of the Doppler shift Equation (1.2). The first is that, from Figure 8 and Figure 10, at locations where the emitter is not abeam, there is separation in the Doppler shifts that can be related to the cross-track distance. This readily correlates with the Doppler equation, as relative velocity between the transmitter and emitter is greater when the satellite velocity aligns closer with the relative position vector. This means that given emitters at varying cross-track distances and equal in-track distances, the closest emitter has the greatest magnitude of Doppler shift at any in-track position except at abeam. This can be identified in Figure 8 by the 700 km range curve having more positive Doppler shift than the other ranges graphed, and in Figure 10 by the 700 km range curve having more negative Doppler shift than the other ranges displayed. At abeam, there is no component of the satellite velocity vector aligned with the relative position vector as they are perpendicular, causing there to be no Doppler shift regardless of cross-track distance. The rate at which the relative velocity changes is also greatest at the abeam point. This can be evidenced by the steeper slope of the Doppler shift curve in Figure 9, which displays the data in close proximity to the abeam point as opposed to the lesser magnitude slopes at locations farther away from the abeam point in Figures 8 and

10. Figures 8–10 all display a one km in-track section in order to make this comparison. From this information, the conclusion can be drawn that the maximum slope and an inflection point occur at the abeam location.

While the concepts can be demonstrated imprecisely from the figures, more precise information can be obtained by using a little math. When the data are evaluated they will be in the form of points, taken at a given sample rate. The first step to make the data easier to use would be to fit a curve to the data. This is easily accomplished through use of any number of programs; MATLAB and a third order curve fit were used for this thesis. The next piece of information that is important to obtain is the location of the maximum slope, or the inflection point, which are collocated in the graph. This can be done by finding the root of the second derivative of the frequency curve (where the first derivative is the slope). The solution of this is the time at which the emitter was abeam the satellite. Assuming that the satellite is at a known location with which the time can be associated, the first of two necessary LOPs for the geolocation can be established. The frequency received at the abeam time is also known to be the base frequency since there is no Doppler shift at that location, as previously discussed.

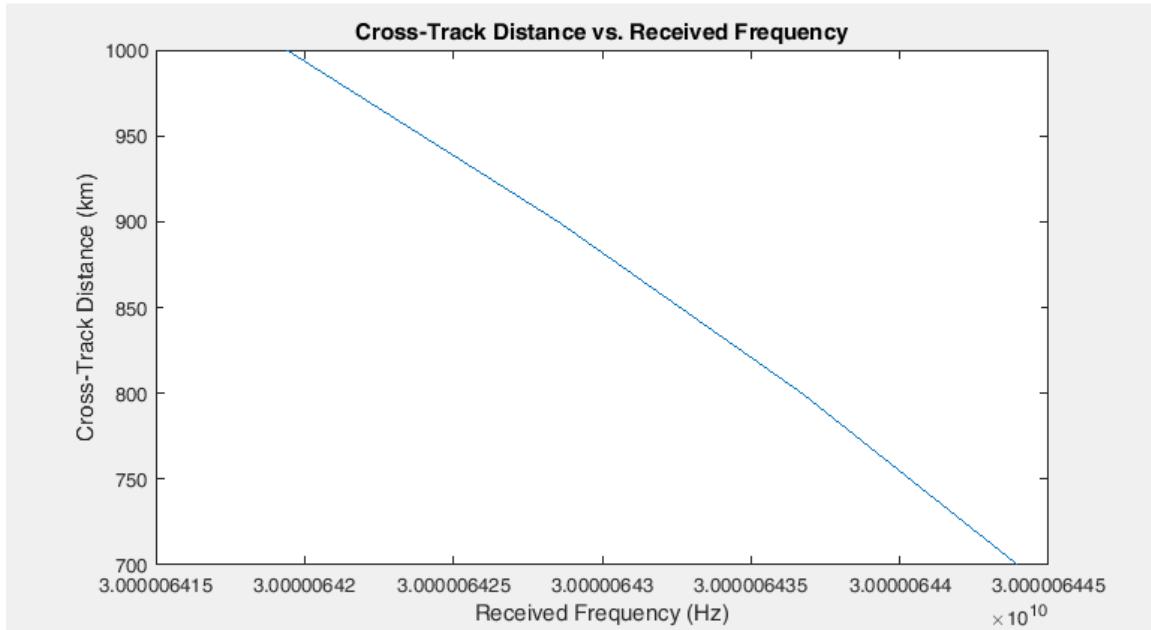
The second LOP will establish the cross-track distance. Now that the base frequency has been calculated, curves can be created which illustrate potential received frequency data from simulated emitters with identical base frequency to the jammer and located at varying cross-track distances, similar to what was done in Figure 7. The difference is that the curves can be tailored to the same extent of time that the emitter frequency data has been collected for and plotted simultaneously against the collected data, with the curves positioned so that the base frequency value on the curve will occur at the abeam time (the curves will all intersect here because of this, similar to Figure 9). For the same scenario as in Figures 8–10, a received frequency curve for a jammer can be simulated at an additional cross track distance (840 km is used for the jammer in Figure 11). The received frequency plots correlating to when the emitter was approximately 1000 km in front of the satellite are shown in Figure 11.

Figure 11. Received Frequency from EMI and Simulated Emitters.



While the point at which the cross-track distance will be interpolated from for the second LOP does not need to be at the farthest distance/time from the abeam point, as in Figure 11, that is where the most separation in frequency occurs between the curves. The cross-track distances cannot be compared at the abeam point as all the curves intersect there, and with no separation in the frequencies the interpolation cannot be performed. Interpolation of a cross-track distance for the jammer is easily done and the results are almost obvious from Figure 11 already. For a fixed in-track distance (or time) data points correlating to the simulated emitters (at known cross-track distances) from the graph are pulled that consist of the frequency received on that curve at the comparison distance/time as the x-value and the cross-track distance of that curve (given in the legend) as a y-value. These values are then plotted and a curve fitted to them, which is Figure 12. From this point the received frequency for the jammer at the comparison distance/time becomes the x-value, and the equation of the best fit line will return the cross track distance.

Figure 12. Graph for Interpolation of Cross-Track LOP.



While the simplified execution of the method for a flat, non-rotating Earth and use of a simulated jammer can be shown to work, a more realistic situation creates numerous challenges that need to be resolved.

B. MODELING

Before addressing adding complexity to the technique, it was necessary to develop a model that would enable accuracy to be checked so that progress in dealing with the added complexity could be tracked. This model would ensure that data generated for the EMI emitter would accurately reflect real-world data, and also that solutions were not inadvertently input to the MATLAB program that was created to perform the geolocation. The modeling was done through the use of Systems Tool Kit (STK), a product of Analytical Graphics, Inc., which allows for highly realistic modeling and simulations to be created and analyzed for a wide variety of situations. STK is used as an analysis tool by both the civil and military space communities and is accepted as an industry standard. In this instance, it was used to analyze the communications link between Earth and space, specifically emitters/jammers and a modeled O3b satellite. Ground-based emitters were placed at various locations to represent the majority of the

O3b coverage area (when considering results for north and south latitudes are symmetrical) in order to provide some insight to performance over varying latitudes/ranges. An O3b satellite model was also created, with the orbit simplified for ease of use as previously discussed. The frequency used for the link was 30 GHz, which is slightly higher than O3b's commercial Ka-band, and falls within the military Ka-band.

STK is able to generate a detailed report on the link budget over time. For modeling the situation for this thesis, the data used was restricted to what would be observable by the satellite if the location of the emitter was not known (for example, no range data for the link was used). The data used consisted of the frequency received by the satellite from the emitter, and a time stamp for each frequency; this was then exported to Microsoft Excel. In Microsoft Excel, the time of each received frequency was modified to be a simple "elapsed time" that simply started at the first point with zero and counted upward at an interval matching the sample rate (which would be known, since that is a function of the satellite monitoring and not the emitter). The MATLAB program would then import the STK-generated data from Microsoft Excel for processing/geolocation. Also entered into the program was the satellite's longitude at the start of the STK scenario. After the program computed the geolocation estimate for the emitter, this was then compared to the actual location of the emitter in STK to evaluate accuracy.

C. ADDING COMPLEXITY

Now that a method and model have been established to track how well complexity is addressed, it is time to increase the realism from the flat, non-rotating Earth, to the real world, which is not flat (or spherical), and is rotating. While the latitude portion of the geolocation solution will change significantly when adding complexity, the other LOP (longitude), must be computed first and changes little from the previously discussed flat, non-rotating Earth scenario. The data used for the geolocation will consist of a time and a received frequency, like the data shown in Table 1. A complete set of data for one modeled emitter can be found in Appendix A. The middle column of Table 1 simply counts the length of time interference has been received, which is an easier format

of time to manipulate/use in the MATLAB program than UTCG. With a non-flat Earth, distance and time are no longer related as simply as in the previous section, because translational velocity of the emitter varies with latitude, which is unknown. This makes it necessary to work with the data as it is referenced to time.

Table 1. Sample Data Excerpt for Geolocation.

Time (UTCG)	Recv Interference Elapsed Time	Rcvd. Frequency (Hz)
-----	-----	-----
29 Mar 2016 20:11:46.000	12	30000042969.19020
29 Mar 2016 20:11:47.000	13	30000042884.06240
29 Mar 2016 20:11:48.000	14	30000042798.91810
29 Mar 2016 20:11:49.000	15	30000042713.75750
29 Mar 2016 20:11:50.000	16	30000042628.58040
29 Mar 2016 20:11:51.000	17	30000042543.38700
29 Mar 2016 20:11:52.000	18	30000042458.17730

The received frequency data are fitted with a curve which is then plotted, much like Figure 9, with the frequency on the y-axis, but now with time on the x-axis instead of distance, as shown in Figure 13. The inflection point of the curve is then found from the second derivative, as was done in the previous scenario. The time at which this inflection point occurs is once again the abeam point, and the received frequency at that time is the base frequency, all based on the previously established concepts. The base frequency will be used later for the comparison curve generation to find the latitude LOP (same process as the cross-track LOP previously). With the abeam time for the emitter identified, the longitude of the satellite at that time (known to the satellite operator or user) is equal to the longitude of the emitter, and the first LOP is complete. The times for the data are then adjusted so that the abeam time is set to zero seconds, and positive time represents time prior to abeam, while negative time will represent data for when the emitter is past the abeam point. This adjustment is somewhat arbitrary, but simplifies comparison to the generated curves for the latitude LOP process as the y-intercept for all curves will be the base frequency. After this adjustment has been completed the resultant graph is shown in Figure 14.

The graph displays a linear relationship between the elapsed time of received interference and the received frequency. The x-axis represents the elapsed time in seconds, ranging from 300 to 650. The y-axis represents the received frequency in Hz, with a scale factor of $\times 10^{10}$ indicated at the top. The frequency starts at approximately 3.0000 $\times 10^{10}$ Hz at 350 seconds and decreases linearly to approximately 3.0000 $\times 10^{10}$ Hz at 650 seconds.

Elapsed Time (s)	Received Frequency (Hz) $\times 10^{10}$
350	3.0000
400	3.0000
450	3.0000
500	3.0000
550	3.0000
600	3.0000
650	3.0000

The graph displays a linear relationship between time and received frequency. The x-axis represents time in seconds relative to the abeam point, ranging from -150 to 200. The y-axis represents the received frequency in Hertz, with a scale factor of 10^{10} , ranging from 3.00000 to 3.00000. A dashed line indicates the frequency sweep, starting at approximately -150 seconds and 3.00000 $\times 10^{10}$ Hz, and ending at approximately 150 seconds and 3.00000 $\times 10^{10}$ Hz.

43

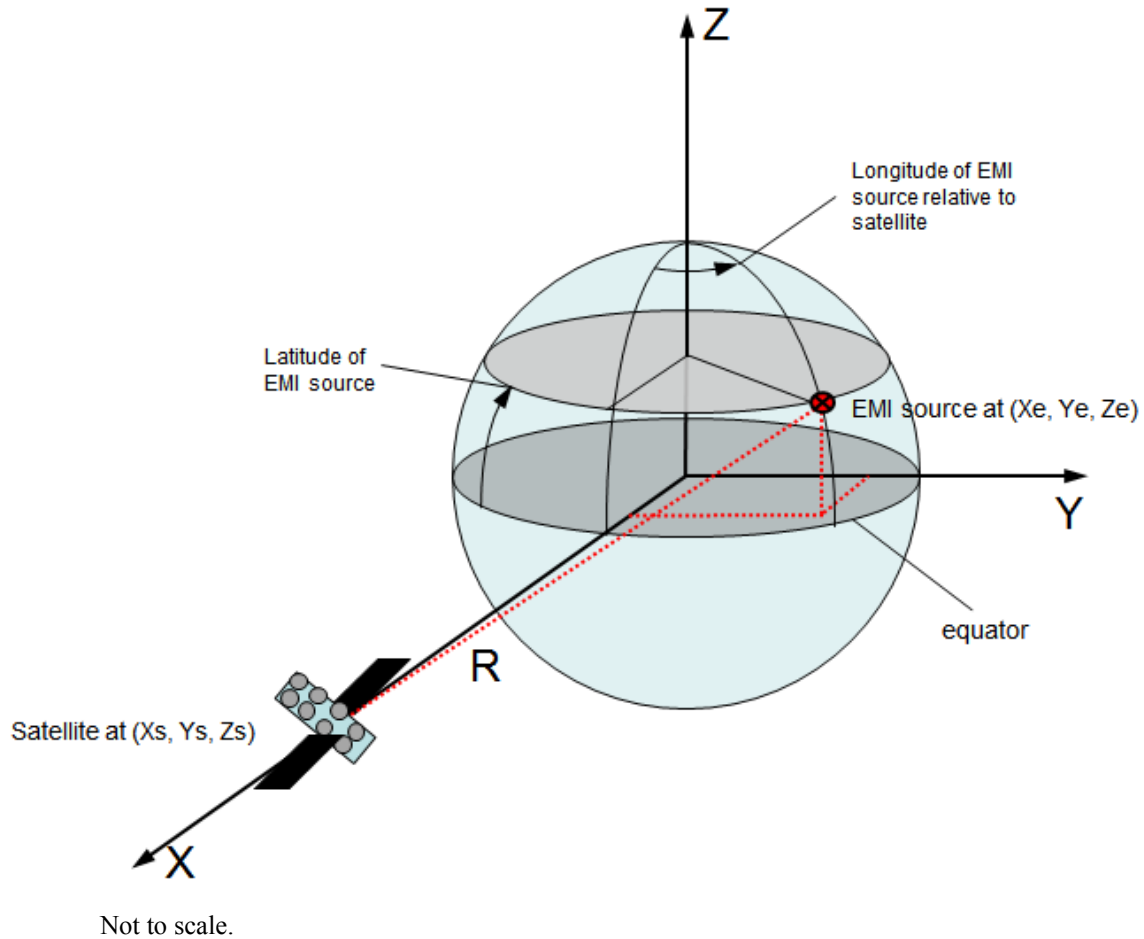
The accuracy of the latitude solution depends on the ability to accurately simulate the received frequency curve of simulated emitters from various, but known locations. This will then be compared to data from the emitter of interest, specifically a graph similar to Figure 14. This will only produce beneficial results if the internally generated data for comparison can mimic what would actually be produced if an emitter was at that location on the Earth, which means that the Earth's shape and rotation must be accounted for.

The first issue is that a different reference system is needed since the Earth's surface is no longer considered flat. Additionally complicating this issue is that the Earth is also not a sphere (the polar axis is shorter than an equatorial axis), and considering it as such would negatively affect results, particularly closer to the poles and locations where the radius would not match that of a spherically modeled Earth. The next issue is that the Earth is rotating, and the rotating Earth results in different velocities of stationary (relative to Earth) emitters at differing latitudes. This is due to the different circumference lengths (when the radii of the circle is measured perpendicular to the polar axis) of different latitudes while all points on the Earth have the same angular velocity. The velocity of emitters varying with latitude matters because Doppler shift is directly related to the relative velocity between the satellite and emitter.

For ease of use, a Cartesian reference system is desirable. In this situation, it will be based at the center of the Earth—because that point does not depend on the Earth's shape. For simplification, the satellite will be considered fixed in the reference system and only the emitter will move, representing all relative motion. This reference system will consist of X in the equatorial plane through the center of the Earth to the satellite, Y perpendicular to X in the equatorial plane, and Z will coincide with the polar axis of the Earth reference ellipsoid. For the satellite, which operates at a fixed altitude (and thus semi-major axis, which will be the “x” coordinate), and is at a constant zero “z” coordinate due to the equatorial orbit, the Cartesian coordinates are simple. Using this reference system also means the “y” coordinate is zero, and Earth referenced longitude does not matter—as long as the satellite's Earth referenced latitude is known at some point during the data collection the change in longitude from the known point can be tracked, for purposes of identifying the emitter's abeam position later. It is also worth

noting that these coordinates are constant over time. This reference system is illustrated in Figure 15.

Figure 15. Reference System.



With the satellite's Cartesian position established, the Cartesian position of simulated emitters must now be calculated in order to determine their relative positions. The emitter's relative position in this reference system changes with time, and because of this velocity becomes a consideration. The emitter is also on the surface of the ellipsoidal Earth and received frequency curves must be calculated for varying latitudes, complicating the computation of coordinates for the emitter more than the satellite. To help address the ellipsoidal Earth issue, instead of creating comparison curves for simulated emitters, similar to Figure 11, identified by cross-track distance in km from the

nadir point of the satellite (700 km, 800 km, etc.), the comparison curves will be referenced to geodetic latitude. In order to use geodetic latitude as a reference while performing the math to generate the data with a Cartesian coordinate system, conversion is necessary. Fortunately, this procedure is detailed in *SMAD*.⁷⁰ The first step is to compute the “ellipsoidal radius of curvature in the meridian,” shown in Equation (1.5), using the semi-major axis of the ellipsoid (a) and the eccentricity of the ellipsoid, (e).⁷¹ This is then used to complete the conversion in Equation (1.5). The additional inputs are “ellipsoidal height” (h), which for an emitter on the surface of Earth will be zero, the geodetic latitude (ϕ), which is known for the curves being generated, and longitude (λ), which will be explained shortly.⁷²

$$N_{\phi} \equiv a / \sqrt{1 - e^2 \sin^2 \phi} \quad [\text{see footnote}]^{73} \quad (1.5)$$

$$\begin{bmatrix} X \\ Y \\ Z \end{bmatrix} = \begin{bmatrix} (N_{\phi} + h) \cos \phi \cos \lambda \\ (N_{\phi} + h) \cos \phi \sin \lambda \\ ((1 - e^2) N_{\phi} + h) \sin \phi \end{bmatrix} \quad [\text{see footnote}]^{74} \quad (1.5)$$

The most useful longitude for this procedure is relative to the satellite’s longitude, as the goal at this point is to generate simulated received frequency data which includes Doppler shift that varies with relative position. Longitude of the emitter relative to the satellite changes with time as a result of both the rotation of the Earth and the orbit of the satellite. A useful way to relate the longitude to time is to use rotational velocity, which is not impacted by the latitude of the emitter as translational velocity would be. The rotational velocity of the satellite relative to the emitter is the difference of the rotational velocity of Earth and the rotational velocity of the satellite in orbit. The difference in rotation velocity coupled with time provides the required relative longitude equation. It is

⁷⁰ Larson and Wertz, *Space Mission Analysis and Design*, 900 (see chap. 1, n. 7).

⁷¹ Ibid.

⁷² Ibid.

⁷³ Ibid.

⁷⁴ Ibid.

important that the equations are variable with time and no other parameters, as time is one of only two data types that result from and can be directly compared to the actual emitter (the other being frequency). The way this technique is applied is that the relative rotational velocity (v_{rot}) in radians/second is calculated as shown in Equation (1.5), where t_s is the satellite's orbital period and t_e is Earth's rotational period (the length of a sidereal day).

$$v_{rot} = \left(\frac{2\pi}{t_s} \right) - \left(\frac{2\pi}{t_e} \right) \quad (1.5)$$

Equation (1.5) does not vary with time, and becomes an input for solving the relative longitude as a function of time. This is done by multiplying v_{rot} by the amount of time ahead or behind the abeam position (which has already been calculated) to output the relative longitude (λ) for conversion to Cartesian coordinates, as shown in Equation (1.5). A quick check for this is that at time (t) = 0 seconds, the relative longitude would also be zero, and therefore be on the same meridian as the satellite.

$$\lambda = v_{rot}t \quad (1.5)$$

With both the satellite and the simulated emitter's locations now known as a function of time, the relative velocity between the two can be calculated. For this, the range will first be calculated using Equation (1.5). This is also shown in Figure 15, denoted by " R ." In the program created, the change in range between the satellite and emitter over a small increment of time (ranges R_1 and R_2) was used to obtain the relative velocity, as shown in Equation (1.5). This velocity then used to obtain the Doppler shifts and added to the base frequency (f), which was found at the abeam position, to obtain received frequency (f_{rec}) curves for the simulated emitters, as shown in Equation (1.5).

$$R = \sqrt{(x_s - x_e)^2 + (y_s - y_e)^2 + (z_s - z_e)^2} \quad (1.5)$$

$$v_{rel} = \frac{\Delta R}{\Delta t} = \frac{(R_1 - R_2)}{\Delta t} \quad (1.5)$$

$$f_{rec} = f + \Delta f = f + \frac{f}{c} v_{rel} \quad (1.5)$$

In this instance, received frequency curves were generated for the simulated emitters at every .5 degrees of latitude from 3.5 degrees below to 3.5 degrees above beam center (the latitude of the beam center would be known by the operator). This approximates latitudes that would be within the BCA, in order to lessen the programming burden. This does not take into account changes in BCA with latitude, but that was not necessary to prove the concept as long as the method could locate emitters away from beam center. Repeating the process, curves could be calculated within the BCA at as small an interval as desired. Adding curves to represent locations farther from beam center would accommodate a larger BCA. For the geolocation to be effective, the comparison curves just need to encompass the possible latitudes of the emitter, as those create the points a curve will be fit to for the interpolation. The comparison curves generated for this instance were based on a beam centered at 57.75° N and are shown in Figure 16. The conditions demonstrated could represent the boresight of the beam aimed at a user located at 57.75° N and the emitter of interest somewhat further from the boresight but still within the BCA. This was done to demonstrate that the emitter of interest (located at 60° N) does not need to be (and presumably often would not be) located perfectly at the center of the BCA for the geolocation method to still be effective.

The next step is to compare the data from the emitter of interest (jammer) in Figure 14 to the comparison curves, as was discussed and done for Figure 11 in the previous section. Figure 17 shows the plot of these curves together, focused on the end of the curves where the separation is most apparent. From the same time value for each of the simulated emitter curves (at known latitudes), data points are taken that consist of the frequency received on that curve at the comparison time as the x-value, and the latitude of the emitter for that curve as a y-value. Figure 18 displays the curve created from these points (latitude is in radians as the program created uses radians for most intermediate steps). The received frequency for the EMI emitter at the comparison time is input as an x-value, and the equation of the best fit line returns the latitude. Results will be discussed in the following chapter.

Figure 16. Received Frequency Curves of Simulated Emitters at Various Latitude.

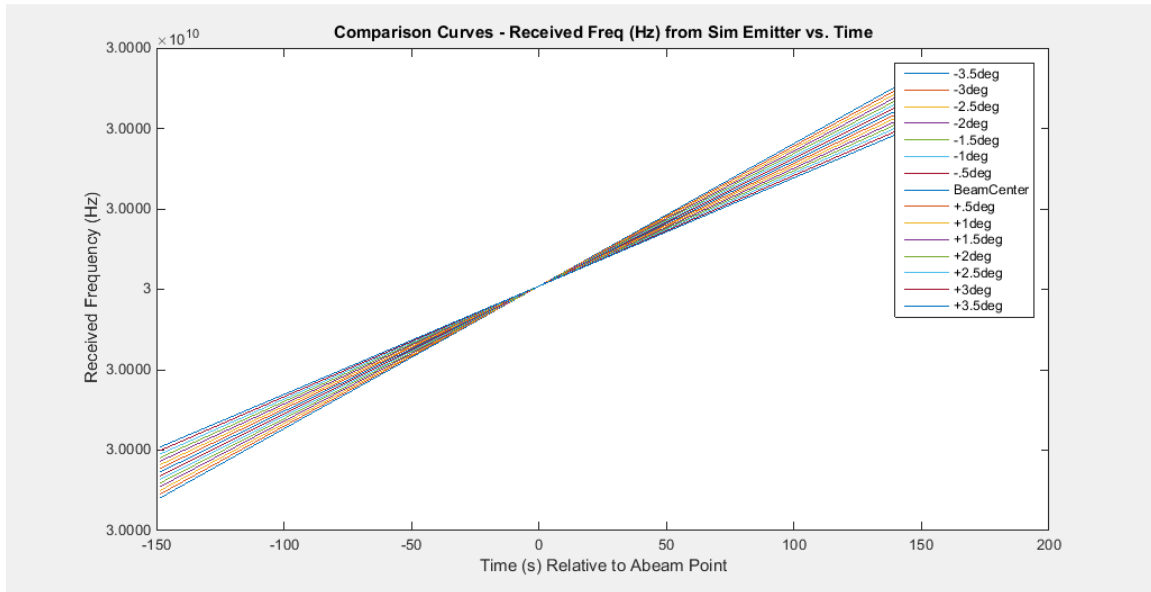


Figure 17. Comparison of Received Frequency between EMI and Simulated Emitters.

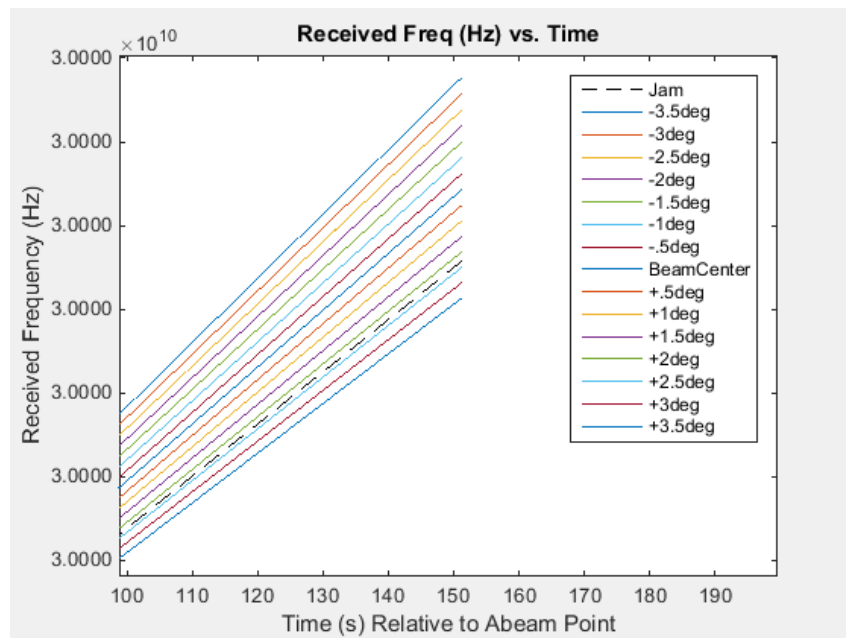
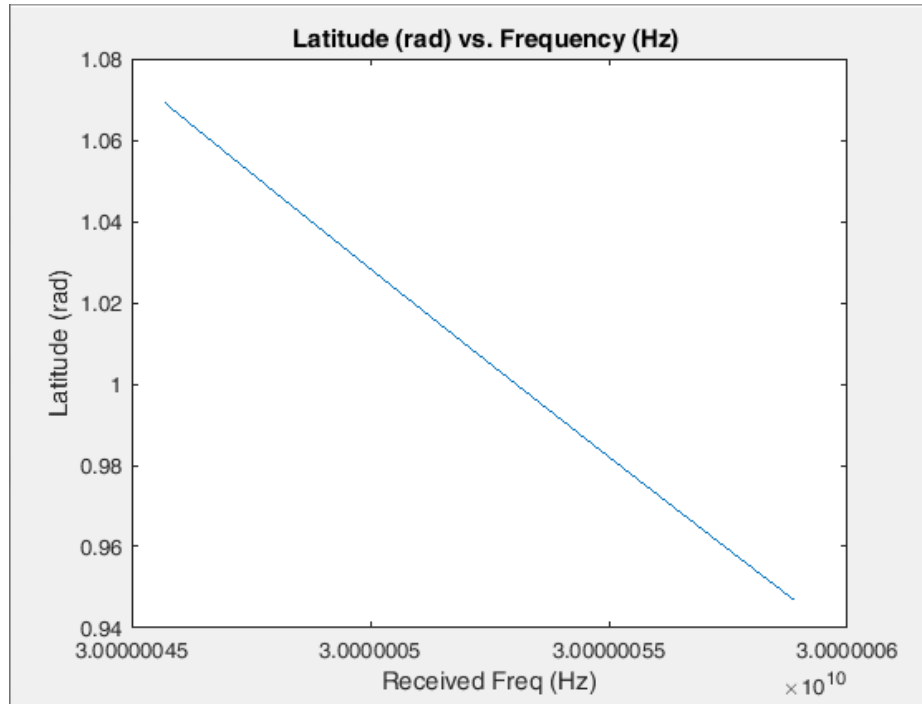


Figure 18. Graph for Interpolation of Latitude of EMI Emitter.



D. CONCLUSION

This chapter developed a technique to take advantage of data that could be obtained and used due to the unique characteristics of O3b's satellites. The result of this technique is the MATLAB program in Appendix B which is capable of outputting a geolocation estimate for input data generated by STK, which models realistic conditions with consideration to the constraints and assumptions addressed at the beginning of the chapter. The next chapter will address the results obtained from this geolocation technique by comparison of the estimated locations of emitters to the actual locations.

V. RESULTS, FUTURE WORK, AND CONCLUSIONS

Now that the technique for the new geolocation method has been developed, the results must be evaluated for accuracy and then analyzed to determine what application or utility they serve in the current form. For evaluation of accuracy with this method latitude and longitude may be analyzed independently because different procedures were used to create their respective LOPs. While a detailed error analysis was not conducted, some possible sources of error are identified. Future work to build on this thesis will also be discussed before concluding this chapter and this thesis.

A. RESULTS

In order to characterize the accuracy of this method through a wide range of possible locations, emitters at 15°N 000°E, 30°N 000°E, 45°N 000°E and 60°N 000°E were modeled in STK and then a geolocation estimate was computed for each emitter using a MATLAB program (see Appendix B). For each of the four emitters an estimated location was computed in three circumstances—one with the emitter at the beam center, one with the beam centered at three degrees latitude below the emitter, and again with the beam centered at three degrees latitude above the emitter. Three degrees latitude from boresight was chosen because the emitter must be within the BCA, and the MATLAB program computes comparison curves out to 3.5 degrees off boresight to simulate the BCA. Three degrees off boresight therefore represents a situation where the emitter would be toward the edge of the BCA, but still within it. To simulate the knowledge a satellite operator would have of the satellite beam's boresight location, and to test accuracy for emitter locations within the BCA but not at the boresight location, the program includes an input for centering the beam at specified latitude. This can be found in Section 1 of the MATLAB program (Appendix B). Section 1 of the program also includes an input for the actual emitter location, which would obviously not be known under normal circumstances, but was used in order to calculate error distances of the estimated emitter location from the actual emitter location, performed in Section 8 of the MATLAB program.

Tables 2–4 display the estimated emitter locations calculated using the geolocation technique, and the distance (km) in error that the estimated positions were from the actual emitter locations for a situation where the emitter falls at the beam’s boresight as well as where it would be at the northern or southern edges of the BCA. The distance used for the error in these tables was calculated by MATLAB for the difference in coordinates between the positions, over the surface of the Earth as represented by an ellipsoid.

Table 2. Actual and Estimated Emitter Locations—Emitter Located at Beam’s Boresight Latitude.

Actual Emitter Position (DD.DDDD)	Estimated Emitter Position (DD.DDDD)	Error Distance (km)
15°N 000°E	15.0513°N 000.0880°W	11.040
30°N 000°E	29.9960°N 000.1175°W	11.348
45°N 000°E	45.0141°N 000.1616°W	12.837
60°N 000°E	60.0445°N 000.2455°W	14.557

Table 3. Actual and Estimated Emitter Locations—Beam’s Boresight 3°S of Emitter Latitude.

Actual Emitter Position (DD.DDDD)	Estimated Emitter Position (DD.DDDD)	Error Distance (km)
15°N 000°E	14.9394°N 000.0880°W	11.601
30°N 000°E	29.9838°N 000.1175°W	11.481
45°N 000°E	45.0246°N 000.1616°W	13.030
60°N 000°E	60.0445°N 000.2455°W	14.557

Table 4. Actual and Estimated Emitter Locations—Beam's Boresight 3°N of Emitter Latitude.

Actual Emitter Position (DD.DDDD)	Estimated Emitter Position (DD.DDDD)	Error Distance (km)
15°N 000°E	14.9394°N 000.0880°W	11.601
30°N 000°E	30.0082°N 000.1175°W	11.375
45°N 000°E	45.0211°N 000.1616°W	12.955
60°N 000°E	60.0585°N 000.2455°W	15.156

These results, for latitudes from 15°N to 60°N (it would be symmetrical for the South) and varying emitter positions within the BCA give a maximum error distance of 15.505 km. One noticeable piece of information from these three tables is that the longitude error for each emitter, at each of the three relative emitter positions within the BCA is the same. For example, the estimated longitude for the emitter actually located at 15°N 000°E, is 000.0880°W for each of Tables 2-4. Since the longitude LOP was also the first LOP calculated during the geolocation technique that will now be discussed in greater depth.

1. Longitude LOP Results

Isolating the longitude LOP from the latitude LOP results in a more clear picture of how accurate the longitude estimation from the geolocation method is and what some of the causes of errors might be at a high level. The longitude LOP error in km is given in Table 5, with the negative symbol representing an estimated position to the west of the actual position. This is a better measure of accuracy than degrees of longitude, as the separation between them varies with latitude. The longitude accuracy can be summarized as having a maximum error of 13.697 km, and an average error of 11.812 km for the latitude ranges tested. The errors show two readily apparent trends, the first being that all the errors are from estimated emitter positions to the west of the actual emitter location. The next trend is that the errors grow larger in magnitude as latitude increases.

Table 5. Longitude LOP Error Analysis.

Position of Emitter	Longitude Error (km)	Error In Estimated Base Frequency (Hz)	Estimated Abeam Time Error (sec) from 0 Hz Doppler Shift Time	Estimated Abeam Time Error (sec) from Satellite LLA Abeam Time
15°N 000°E	-9.468	16.132	-0.18	-1.48
30°N 000°E	-11.339	32.524	-0.45	-3.25
45°N 000°E	-12.743	53.559	-1.06	-5.90
60°N 000°E	-13.697	79.197	-2.54	-10.93

The longitude LOP was created by finding the inflection point on the received frequency curve, which was created using the frequency of the received interference over the associated time. This was done to find the base frequency of the emitter and the time at which that base frequency was received, which equates to when the Doppler shift would be zero and the emitter would be abeam (abeam time). For a longitude LOP error to occur, it would be a result of an error in those prior steps.

The first thing that was found in further analysis was that there was an error in the MATLAB program's ability to calculate the base frequency, and the time at which it occurred. It is possible that an increased sample rate of the emitter frequency could help this computation, but that analysis was not conducted during this thesis. The MATLAB calculated base frequency error is shown in Table 5, with the positive denoting that the frequency calculated was above the actual base frequency of 30 GHz. Table 5 also shows the error in the time between where MATLAB calculated the time of the inflection point, as compared to the time in the raw frequency data that the Doppler shift became zero. The negative for this column denotes that the MATLAB calculated inflection point occurred earlier than the actual Doppler shift in the data became zero. Both the calculated frequency and error in the abeam time increased as the latitude of the emitter increased, just as the position error does. With a maximum error of less than three seconds however, and a relative rotation velocity between the satellite and the emitter of .017 degrees/sec, the maximum longitude error would be less than .051 degrees. This meant that the error could not be fully attributed to this.

The emitters were also all located along the same meridian (Prime Meridian), and therefore the abeam time and the time at which the Doppler shift became zero should not have varied with the emitters' latitudes. In comparing the time at which the Doppler shift became zero in the STK generated report to the time at which the satellite modeled in STK crossed the Prime Meridian, an additional discrepancy was discovered. The time at which the satellite was at 0°E according to the latitude, longitude, altitude (LLA) coordinates displayed within STK differed significantly in each instance from the time at which the Doppler shift was zero. In each case the time at which the Doppler shift was at zero was earlier than the satellite's longitude was 0°E, and the difference grew significantly for the emitters at higher latitudes. While there is a difference in range between the various emitters and the satellite, the difference in range (around 4000 km) is far too small for the speed of light and transit time for the signal (difference of about .01 seconds, increased from .03 to .04 seconds total) to account for the time differences. This time difference compounded the error between the MATLAB calculated abeam time and the zero Doppler shift time, resulting in the time differences shown in the final column of Table 5. It is unclear the reason for the differences in times, but they are undoubtedly a significant contributor to the error in longitude. At this time, additional analysis would be needed to understand this error, and testing would be useful to determine if it is a result only of the modeling used in STK or if the same time discrepancies would occur under actual conditions. If the error discussed were to be consistent with operational testing results, it could be characterized over the full range of latitudes and then corrected for.

2. Latitude LOP Results

The error in km resulting from the latitude LOP compared with the latitude of the actual emitter is given in Table 6, where a negative sign represents that the estimated position was south of the actual position. The maximum error was 6.702 km, with an average error distance of 3.776 km. These results show that the estimations for the 30°N emitter were always the most accurate. This was followed by the 45°N emitter. The 45°N and 60°N emitter locations were always South of the estimated location regardless of where in the BCA the emitter was placed. The 15°N and 30°N latitude estimates were not consistently to the North or South of the actual emitter.

Table 6. Latitude LOP Error Analysis.

Position of Emitter	Latitude Error (km) Emitter at Boresight	Latitude Error (km) Boresight 3°S of Emitter	Latitude Error (km) Boresight 3°N of Emitter
15°N 000°E	5.680	-6.702	-6.702
30°N 000°E	-0.443	-1.800	0.914
45°N 000°E	1.569	2.735	2.346
60°N 000°E	4.954	4.954	6.513

The latitude LOP was calculated from the comparison of the received frequency of the emitter to the generated curves for simulated emitters at various assigned latitudes. The only input to the generated curves tied to the actual emitter was the calculated base frequency based on the inflection point/abeam time calculation previously discussed. The error in frequency, which was previously shown in Table 5, is therefore a potential source of error. Another factor in generating the curves for comparison is the conversion of geodetic latitude to Cartesian coordinates, which uses an ellipsoid to represent the Earth. While this model is extremely useful, it is doubtful that it perfectly represents the actual Earth, or the STK model of Earth that generated the frequency data for the actual emitter to be located. The ellipsoid model could very well be the most reasonable explanation for the fact that the mid-latitudes were consistently the most accurate, if that is where the ellipsoid used most accurately represents the STK model (in this case) or the real world. There exists very accurate models of the Earth's shape, and incorporation of one into the geolocation program could provide improved accuracy over the ellipsoidal model used.

For the comparison curve generation, in the current version of the program they are spaced at .5° latitude increments and only created for 3.5°S to 3.5°N of the beam's boresight latitude. Creation of more of these curves and spacing them closer together would provide more points for the interpolation step which estimates the emitter's latitude. In the current method there are 15 points that a curve is then fit to. More points could result in a more precise curve fit and better latitude estimation, although it does appear to be smooth and already well characterized by the curve. The results did not show noticeable trends based on where the emitter was placed inside the BCA, which is positive feedback for the geolocation method and one of the reasons for associating the

comparison curves with geodetic latitudes. The comparison curves also do not need to be limited to within the BCA; they could be computed as close together as desired from the equator to the northern extent of the coverage area. Doing so may not increase accuracy if there are sufficient curves computed within the BCA. While it was not demonstrated in these results, what also must be remembered with respect to the BCA is that the beam's position (north or south) is being used to resolve ambiguity between symmetrical latitudes, so if the satellite's beam was centered on the equator there would be two possible latitudes of the emitter. In that case, it is possible that a slight satellite inclination would result in a unique location, but that fell outside the scope of this thesis.

3. Conclusion

The errors for the latitude and longitude LOPs are summarized in Table 7. While steps could be taken to improve the accuracy of both processes, some insight has been provided for where those errors seem to originate. Currently, the latitude LOP seems to be significantly more accurate than the longitude LOP. The longitude LOP accuracy is significantly impacted by the timing issue discussed, which may be a symptom of the modeling conducted and not persist under actual conditions, and could be corrected for. Without further correction for either method, the results do prove that the new method is a viable means of conducting geolocation of EMI emitters using O3b satellites.

Table 7. Magnitude of Error Summary for Latitude and Longitude.

	Magnitude of Avg. Error in km	Magnitude of Max. Error in km	Magnitude of Min. Error in km
Latitude LOP	3.776	6.702	0.443
Longitude LOP	11.812	13.697	9.468

B. UTILITY OF THE GEOLOCATION METHOD

The results discussed serve as proof of concept for the geolocation technique. While accuracy could be improved, in the current form the results would still prove useful to the DOD, or for that matter, any user of O3b satellite communications. The usefulness of the technique at the current accuracy level will be discussed in this section.

Two steps of the JSIR process are characterization of the interference source, and geolocation.⁷⁵ Use of this method could help determine whether the interfering source is friendly and interference is unintentional, or it is hostile and intentional. In the case where the interfering source location is associated with friendly units, the method could provide insight as to which unit or base the interference is coming from. In the event the interference is intentional, it could provide intelligence on adversary capabilities or support networks used to acquire the interference equipment. If in a complicated area of operations with multiple actors, the geolocation method could place the location inside territory controlled by one of them, again providing useful knowledge. In the event the interference appears to be the result of a state actor, it could enable diplomatic actions to be taken to cease the interference.

If the interference cannot be stopped at the source, a simple way interference can be resolved is to re-point the BCA containing the interference such that the interfering source is inside a null of the antenna. The narrow beam width is one of the advantages of Ka-band, which can be used for exactly this purpose. While there is significant gain out to the -6 dB point in the O3b payload antenna receive pattern, beyond that the gain drops off sharply, as was shown in Figure 1 and Figure 4. Moving the beam slightly can place the interfering source into this disadvantageous null in the pattern while maintaining the user in the higher gain of the beam pattern.

While the level of accuracy achieved by this method is useful on its own, it can also be enhanced by using other knowledge and situations that may be applicable. An example is that if the location area includes water, it may be more likely that the interfering source is located on the land nearby. Another situation would be that if there

⁷⁵ “Joint Spectrum Interference Resolution (JSIR) Procedures,” A-6 (see chap. 1, n. 14).

have been interfering sources that were previously located by more accurate means, a location area including that source location could possibly be assumed to be a repeat offense by the same source. In a remote area, there may be little development which could hide an interfering antenna/source. Finally, the United States or its allies may have assets capable of providing a more accurate location of the interfering source. The initial estimate provided by the geolocation method developed may allow these other assets to focus their search area so that they may be used most efficiently, ensuring they are available for other tasking as soon as possible. If the worst case geolocation is conservatively considered to have a radius for a circular area of probability (AOP) of 20 km, and the BCA where the emitter can be assumed to be located has a radius of 350 km, the area needed to be searched by more capable assets has been reduced by 99.7% through use of this method, greatly increasing their efficiency for what is likely a low density asset. While any of these supplementary procedures are pending or taking place, O3b can easily restore communications by beam steering, as discussed in the previous paragraph.

C. FUTURE WORK

While this thesis did achieve a proof of concept for a new geolocation method in Ka-band using O3b satellites, there is still opportunity for further refinement. The first of these opportunities is to conduct a sensitivity analysis that would identify the largest causes of errors. Among known errors and areas for refinement is the ability of the program to calculate the base frequency of the transmitter from the second derivative of the received frequency curve. This error, with the abeam time calculation, results in a portion of the error in the longitude LOP calculation. A much larger portion of the error was traced back to STK and a time discrepancy between when the satellite was abeam the emitter and the time at which the Doppler shift went to zero, with no apparent cause, warranting further research. For the latitude LOP, creating additional comparison curves and optimizing the curve fit for the interpolation curve resulting from the added points may result in improved accuracy. Along with error resolution/accuracy enhancement should be adding the last increment of realism to the modeling, which would involve using the O3b satellite ephemeris data instead of the simplified orbit at 0° inclination and

no eccentricity. In addition to this, this thesis has assumed that the carrier frequency of the interfering signal can be monitored to the same level of precision simulated by the STK scenario. While O3b Networks does use carrier monitoring software at gateway locations, further research would be needed to see if this currently provides the data necessary to implement use of this geolocation method.⁷⁶ If the current system does not provide the data necessary, then signal processing may be necessary to obtain the data required for practical use. Actual testing of the method would also be a necessary step before implementation could be considered. Testing could then enable a thorough error analysis under realistic conditions and not under the constraints of modeling, and appropriate calibration applied to optimize use of the method.

While not directly related to this method, a different approach to using O3b satellites to perform the geolocation was briefly discussed with thesis advisors. This would involve treating the geolocation as a general estimation problem, which could then be solved using an iterative method (such as the Newton-Raphson method). Due to time constraints this approach was not pursued, but it could be an alternative to the developed method and provide the same benefits of availability and low cost with a useful level of accuracy.

D. CONCLUSION

For the DOD this geolocation method has great potential. Likely the two greatest benefits to the DOD are cost and availability. This method can be executed using MATLAB, Microsoft Excel, and an inexpensive laptop, all of which could be made readily available by units in the DOD. These can be reasonably assumed to be lower cost than a dedicated signals intelligence (SIGINT) or electronic warfare (EW) asset providing geolocation capability. The cost of a laptop with the identified programs might run hundreds of dollars, whereas a single plane could cost millions of dollars, and for a satellite, hundreds of millions of dollars. Furthermore, there is no risk involved, as no asset needs to be deployed to conduct the geolocation unless additional accuracy is desired. The only input necessary for the method to work is a received frequency and

⁷⁶ Ken Mentasti, email message to author, February 1, 2016.

associated time, which would already be monitored by O3b Networks or/and the customer. Use of O3b for communications would presumably already be paid for, as the DOD would not be concerned if an O3b satellite experienced jamming unless the DOD was the customer. O3b Networks may even desire to implement the geolocation method in order to provide customers better service by mitigation of interference using beam steering. If the method was implemented by the company instead of the DOD, then the ability to obtain the geolocation from them to gain any potential intelligence benefit from it could surely be worked out. The accuracy in the method's current form is enough to be useful, but may not be an improvement over existing abilities. While that is true, an asset that is capable of greater accuracy but not available to the user at the time interference occurs, is not useful at all. The new geolocation method does require for the satellite to pass abeam the emitter before the geolocation can be obtained, which does take time but is likely still faster than a more capable (and typically expensive and scarce) asset could be tasked. The timeliness of this geolocation would also not depend on the unit's priority for the tasking of the more capable asset.

This geolocation method could become an organic, low cost, 100% available capability to any unit with the ability to run the received frequency and time data of the interference source through the MATLAB program. The timeliness of obtaining an estimate for the emitter location would only depend on how long it took for the satellite to transit abeam the emitter. The accuracy is currently enough to mitigate the interference and possibly provide useful intelligence, with the potential for the accuracy to be increased beyond the current state. These are substantial benefits to the DOD which are currently not provided by other means and are worth pursuing—particularly in light of the crucial role SATCOM plays for the DOD and the growing use of Ka-band frequencies in that role.

THIS PAGE INTENTIONALLY LEFT BLANK

APPENDIX A. SAMPLE DATA FOR USE IN MATLAB PROGRAM

Table 8. STK Generated Data for Emitter at 30°N 000°E.

Time (UTCG)	Recv Interference Elapsed Time	Rcvd. Frequency (Hz)
-----	-----	-----
29 Mar 2016 20:17:20.000	347	30000010947.08560
29 Mar 2016 20:17:21.000	348	30000010875.94140
29 Mar 2016 20:17:22.000	349	30000010804.79390
29 Mar 2016 20:17:23.000	350	30000010733.64300
29 Mar 2016 20:17:24.000	351	30000010662.48870
29 Mar 2016 20:17:25.000	352	30000010591.33120
29 Mar 2016 20:17:26.000	353	30000010520.17040
29 Mar 2016 20:17:27.000	354	30000010449.00630
29 Mar 2016 20:17:28.000	355	30000010377.83910
29 Mar 2016 20:17:29.000	356	30000010306.66860
29 Mar 2016 20:17:30.000	357	30000010235.49490
29 Mar 2016 20:17:31.000	358	30000010164.31810
29 Mar 2016 20:17:32.000	359	30000010093.13810
29 Mar 2016 20:17:33.000	360	30000010021.95500
29 Mar 2016 20:17:34.000	361	30000009950.76880
29 Mar 2016 20:17:35.000	362	30000009879.57950
29 Mar 2016 20:17:36.000	363	30000009808.38720
29 Mar 2016 20:17:37.000	364	30000009737.19180
29 Mar 2016 20:17:38.000	365	30000009665.99340
29 Mar 2016 20:17:39.000	366	30000009594.79210
29 Mar 2016 20:17:40.000	367	30000009523.58770
29 Mar 2016 20:17:41.000	368	30000009452.38050
29 Mar 2016 20:17:42.000	369	30000009381.17030
29 Mar 2016 20:17:43.000	370	30000009309.95720
29 Mar 2016 20:17:44.000	371	30000009238.74120
29 Mar 2016 20:17:45.000	372	30000009167.52240
29 Mar 2016 20:17:46.000	373	30000009096.30070
29 Mar 2016 20:17:47.000	374	30000009025.07620
29 Mar 2016 20:17:48.000	375	30000008953.84890
29 Mar 2016 20:17:49.000	376	30000008882.61890
29 Mar 2016 20:17:50.000	377	30000008811.38610
29 Mar 2016 20:17:51.000	378	30000008740.15060
29 Mar 2016 20:17:52.000	379	30000008668.91240
29 Mar 2016 20:17:53.000	380	30000008597.67150

29 Mar 2016 20:17:54.000	381	30000008526.42790
29 Mar 2016 20:17:55.000	382	30000008455.18170
29 Mar 2016 20:17:56.000	383	30000008383.93290
29 Mar 2016 20:17:57.000	384	30000008312.68150
29 Mar 2016 20:17:58.000	385	30000008241.42760
29 Mar 2016 20:17:59.000	386	30000008170.17110
29 Mar 2016 20:18:00.000	387	30000008098.91200
29 Mar 2016 20:18:01.000	388	30000008027.65050
29 Mar 2016 20:18:02.000	389	30000007956.38640
29 Mar 2016 20:18:03.000	390	30000007885.11990
29 Mar 2016 20:18:04.000	391	30000007813.85100
29 Mar 2016 20:18:05.000	392	30000007742.57970
29 Mar 2016 20:18:06.000	393	30000007671.30590
29 Mar 2016 20:18:07.000	394	30000007600.02980
29 Mar 2016 20:18:08.000	395	30000007528.75140
29 Mar 2016 20:18:09.000	396	30000007457.47060
29 Mar 2016 20:18:10.000	397	30000007386.18750
29 Mar 2016 20:18:11.000	398	30000007314.90210
29 Mar 2016 20:18:12.000	399	30000007243.61450
29 Mar 2016 20:18:13.000	400	30000007172.32460
29 Mar 2016 20:18:14.000	401	30000007101.03250
29 Mar 2016 20:18:15.000	402	30000007029.73820
29 Mar 2016 20:18:16.000	403	30000006958.44170
29 Mar 2016 20:18:17.000	404	30000006887.14310
29 Mar 2016 20:18:18.000	405	30000006815.84230
29 Mar 2016 20:18:19.000	406	30000006744.53950
29 Mar 2016 20:18:20.000	407	30000006673.23460
29 Mar 2016 20:18:21.000	408	30000006601.92760
29 Mar 2016 20:18:22.000	409	30000006530.61850
29 Mar 2016 20:18:23.000	410	30000006459.30740
29 Mar 2016 20:18:24.000	411	30000006387.99440
29 Mar 2016 20:18:25.000	412	30000006316.67930
29 Mar 2016 20:18:26.000	413	30000006245.36240
29 Mar 2016 20:18:27.000	414	30000006174.04350
29 Mar 2016 20:18:28.000	415	30000006102.72260
29 Mar 2016 20:18:29.000	416	30000006031.39990
29 Mar 2016 20:18:30.000	417	30000005960.07540
29 Mar 2016 20:18:31.000	418	30000005888.74890
29 Mar 2016 20:18:32.000	419	30000005817.42070
29 Mar 2016 20:18:33.000	420	30000005746.09070

29 Mar 2016 20:18:34.000	421	30000005674.75880
29 Mar 2016 20:18:35.000	422	30000005603.42530
29 Mar 2016 20:18:36.000	423	30000005532.09000
29 Mar 2016 20:18:37.000	424	30000005460.75300
29 Mar 2016 20:18:38.000	425	30000005389.41430
29 Mar 2016 20:18:39.000	426	30000005318.07390
29 Mar 2016 20:18:40.000	427	30000005246.73190
29 Mar 2016 20:18:41.000	428	30000005175.38830
29 Mar 2016 20:18:42.000	429	30000005104.04310
29 Mar 2016 20:18:43.000	430	30000005032.69630
29 Mar 2016 20:18:44.000	431	30000004961.34800
29 Mar 2016 20:18:45.000	432	30000004889.99810
29 Mar 2016 20:18:46.000	433	30000004818.64670
29 Mar 2016 20:18:47.000	434	30000004747.29380
29 Mar 2016 20:18:48.000	435	30000004675.93950
29 Mar 2016 20:18:49.000	436	30000004604.58370
29 Mar 2016 20:18:50.000	437	30000004533.22650
29 Mar 2016 20:18:51.000	438	30000004461.86790
29 Mar 2016 20:18:52.000	439	30000004390.50790
29 Mar 2016 20:18:53.000	440	30000004319.14650
29 Mar 2016 20:18:54.000	441	30000004247.78390
29 Mar 2016 20:18:55.000	442	30000004176.41990
29 Mar 2016 20:18:56.000	443	30000004105.05460
29 Mar 2016 20:18:57.000	444	30000004033.68810
29 Mar 2016 20:18:58.000	445	30000003962.32030
29 Mar 2016 20:18:59.000	446	30000003890.95130
29 Mar 2016 20:19:00.000	447	30000003819.58110
29 Mar 2016 20:19:01.000	448	30000003748.20970
29 Mar 2016 20:19:02.000	449	30000003676.83720
29 Mar 2016 20:19:03.000	450	30000003605.46350
29 Mar 2016 20:19:04.000	451	30000003534.08880
29 Mar 2016 20:19:05.000	452	30000003462.71290
29 Mar 2016 20:19:06.000	453	30000003391.33600
29 Mar 2016 20:19:07.000	454	30000003319.95800
29 Mar 2016 20:19:08.000	455	30000003248.57900
29 Mar 2016 20:19:09.000	456	30000003177.19900
29 Mar 2016 20:19:10.000	457	30000003105.81800
29 Mar 2016 20:19:11.000	458	30000003034.43610
29 Mar 2016 20:19:12.000	459	30000002963.05320
29 Mar 2016 20:19:13.000	460	30000002891.66940

29 Mar 2016 20:19:14.000	461	30000002820.28480
29 Mar 2016 20:19:15.000	462	30000002748.89920
29 Mar 2016 20:19:16.000	463	30000002677.51280
29 Mar 2016 20:19:17.000	464	30000002606.12560
29 Mar 2016 20:19:18.000	465	30000002534.73760
29 Mar 2016 20:19:19.000	466	30000002463.34890
29 Mar 2016 20:19:20.000	467	30000002391.95930
29 Mar 2016 20:19:21.000	468	30000002320.56910
29 Mar 2016 20:19:22.000	469	30000002249.17810
29 Mar 2016 20:19:23.000	470	30000002177.78640
29 Mar 2016 20:19:24.000	471	30000002106.39410
29 Mar 2016 20:19:25.000	472	30000002035.00110
29 Mar 2016 20:19:26.000	473	30000001963.60750
29 Mar 2016 20:19:27.000	474	30000001892.21330
29 Mar 2016 20:19:28.000	475	30000001820.81850
29 Mar 2016 20:19:29.000	476	30000001749.42310
29 Mar 2016 20:19:30.000	477	30000001678.02730
29 Mar 2016 20:19:31.000	478	30000001606.63090
29 Mar 2016 20:19:32.000	479	30000001535.23400
29 Mar 2016 20:19:33.000	480	30000001463.83670
29 Mar 2016 20:19:34.000	481	30000001392.43890
29 Mar 2016 20:19:35.000	482	30000001321.04070
29 Mar 2016 20:19:36.000	483	30000001249.64200
29 Mar 2016 20:19:37.000	484	30000001178.24310
29 Mar 2016 20:19:38.000	485	30000001106.84370
29 Mar 2016 20:19:39.000	486	30000001035.44400
29 Mar 2016 20:19:40.000	487	30000000964.04400
29 Mar 2016 20:19:41.000	488	30000000892.64380
29 Mar 2016 20:19:42.000	489	30000000821.24320
29 Mar 2016 20:19:43.000	490	30000000749.84240
29 Mar 2016 20:19:44.000	491	30000000678.44140
29 Mar 2016 20:19:45.000	492	30000000607.04020
29 Mar 2016 20:19:46.000	493	30000000535.63880
29 Mar 2016 20:19:47.000	494	30000000464.23720
29 Mar 2016 20:19:48.000	495	30000000392.83550
29 Mar 2016 20:19:49.000	496	30000000321.43370
29 Mar 2016 20:19:50.000	497	30000000250.03180
29 Mar 2016 20:19:51.000	498	30000000178.62990
29 Mar 2016 20:19:52.000	499	30000000107.22790
29 Mar 2016 20:19:53.000	500	30000000035.82580

29 Mar 2016 20:19:54.000	501	29999999964.42380
29 Mar 2016 20:19:55.000	502	299999999893.02180
29 Mar 2016 20:19:56.000	503	299999999821.61980
29 Mar 2016 20:19:57.000	504	299999999750.21790
29 Mar 2016 20:19:58.000	505	299999999678.81610
29 Mar 2016 20:19:59.000	506	299999999607.41440
29 Mar 2016 20:20:00.000	507	299999999536.01290
29 Mar 2016 20:20:01.000	508	299999999464.61140
29 Mar 2016 20:20:02.000	509	299999999393.21020
29 Mar 2016 20:20:03.000	510	299999999321.80920
29 Mar 2016 20:20:04.000	511	299999999250.40830
29 Mar 2016 20:20:05.000	512	299999999179.00780
29 Mar 2016 20:20:06.000	513	299999999107.60750
29 Mar 2016 20:20:07.000	514	299999999036.20740
29 Mar 2016 20:20:08.000	515	299999998964.80770
29 Mar 2016 20:20:09.000	516	299999998893.40830
29 Mar 2016 20:20:10.000	517	299999998822.00930
29 Mar 2016 20:20:11.000	518	299999998750.61070
29 Mar 2016 20:20:12.000	519	299999998679.21240
29 Mar 2016 20:20:13.000	520	299999998607.81460
29 Mar 2016 20:20:14.000	521	299999998536.41720
29 Mar 2016 20:20:15.000	522	299999998465.02030
29 Mar 2016 20:20:16.000	523	299999998393.62380
29 Mar 2016 20:20:17.000	524	299999998322.22790
29 Mar 2016 20:20:18.000	525	299999998250.83250
29 Mar 2016 20:20:19.000	526	299999998179.43770
29 Mar 2016 20:20:20.000	527	299999998108.04340
29 Mar 2016 20:20:21.000	528	299999998036.64980
29 Mar 2016 20:20:22.000	529	299999997965.25670
29 Mar 2016 20:20:23.000	530	299999997893.86430
29 Mar 2016 20:20:24.000	531	299999997822.47260
29 Mar 2016 20:20:25.000	532	299999997751.08150
29 Mar 2016 20:20:26.000	533	299999997679.69120
29 Mar 2016 20:20:27.000	534	299999997608.30160
29 Mar 2016 20:20:28.000	535	299999997536.91270
29 Mar 2016 20:20:29.000	536	299999997465.52470
29 Mar 2016 20:20:30.000	537	299999997394.13740
29 Mar 2016 20:20:31.000	538	299999997322.75090
29 Mar 2016 20:20:32.000	539	299999997251.36530
29 Mar 2016 20:20:33.000	540	299999997179.98060

29 Mar 2016 20:20:34.000	541	29999997108.59670
29 Mar 2016 20:20:35.000	542	29999997037.21370
29 Mar 2016 20:20:36.000	543	29999996965.83170
29 Mar 2016 20:20:37.000	544	29999996894.45060
29 Mar 2016 20:20:38.000	545	29999996823.07050
29 Mar 2016 20:20:39.000	546	29999996751.69140
29 Mar 2016 20:20:40.000	547	29999996680.31340
29 Mar 2016 20:20:41.000	548	29999996608.93630
29 Mar 2016 20:20:42.000	549	29999996537.56040
29 Mar 2016 20:20:43.000	550	29999996466.18550
29 Mar 2016 20:20:44.000	551	29999996394.81170
29 Mar 2016 20:20:45.000	552	29999996323.43910
29 Mar 2016 20:20:46.000	553	29999996252.06760
29 Mar 2016 20:20:47.000	554	29999996180.69730
29 Mar 2016 20:20:48.000	555	29999996109.32810
29 Mar 2016 20:20:49.000	556	29999996037.96030
29 Mar 2016 20:20:50.000	557	29999995966.59360
29 Mar 2016 20:20:51.000	558	29999995895.22820
29 Mar 2016 20:20:52.000	559	29999995823.86410
29 Mar 2016 20:20:53.000	560	29999995752.50130
29 Mar 2016 20:20:54.000	561	29999995681.13980
29 Mar 2016 20:20:55.000	562	29999995609.77970
29 Mar 2016 20:20:56.000	563	29999995538.42100
29 Mar 2016 20:20:57.000	564	29999995467.06370
29 Mar 2016 20:20:58.000	565	29999995395.70770
29 Mar 2016 20:20:59.000	566	29999995324.35330
29 Mar 2016 20:21:00.000	567	29999995253.00020
29 Mar 2016 20:21:01.000	568	29999995181.64870
29 Mar 2016 20:21:02.000	569	29999995110.29870
29 Mar 2016 20:21:03.000	570	29999995038.95020
29 Mar 2016 20:21:04.000	571	29999994967.60320
29 Mar 2016 20:21:05.000	572	29999994896.25790
29 Mar 2016 20:21:06.000	573	29999994824.91410
29 Mar 2016 20:21:07.000	574	29999994753.57190
29 Mar 2016 20:21:08.000	575	29999994682.23140
29 Mar 2016 20:21:09.000	576	29999994610.89260
29 Mar 2016 20:21:10.000	577	29999994539.55540
29 Mar 2016 20:21:11.000	578	29999994468.22000
29 Mar 2016 20:21:12.000	579	29999994396.88620
29 Mar 2016 20:21:13.000	580	29999994325.55420

29 Mar 2016 20:21:14.000	581	29999994254.22400
29 Mar 2016 20:21:15.000	582	29999994182.89560
29 Mar 2016 20:21:16.000	583	29999994111.56910
29 Mar 2016 20:21:17.000	584	29999994040.24430
29 Mar 2016 20:21:18.000	585	29999993968.92140
29 Mar 2016 20:21:19.000	586	29999993897.60040
29 Mar 2016 20:21:20.000	587	29999993826.28130
29 Mar 2016 20:21:21.000	588	29999993754.96410
29 Mar 2016 20:21:22.000	589	29999993683.64890
29 Mar 2016 20:21:23.000	590	29999993612.33570
29 Mar 2016 20:21:24.000	591	29999993541.02440
29 Mar 2016 20:21:25.000	592	29999993469.71520
29 Mar 2016 20:21:26.000	593	29999993398.40800
29 Mar 2016 20:21:27.000	594	29999993327.10280
29 Mar 2016 20:21:28.000	595	29999993255.79980
29 Mar 2016 20:21:29.000	596	29999993184.49880
29 Mar 2016 20:21:30.000	597	29999993113.20000
29 Mar 2016 20:21:31.000	598	29999993041.90340
29 Mar 2016 20:21:32.000	599	29999992970.60880
29 Mar 2016 20:21:33.000	600	29999992899.31650
29 Mar 2016 20:21:34.000	601	29999992828.02640
29 Mar 2016 20:21:35.000	602	29999992756.73860
29 Mar 2016 20:21:36.000	603	29999992685.45300
29 Mar 2016 20:21:37.000	604	29999992614.16970
29 Mar 2016 20:21:38.000	605	29999992542.88870
29 Mar 2016 20:21:39.000	606	29999992471.61000
29 Mar 2016 20:21:40.000	607	29999992400.33360
29 Mar 2016 20:21:41.000	608	29999992329.05970
29 Mar 2016 20:21:42.000	609	29999992257.78810
29 Mar 2016 20:21:43.000	610	29999992186.51900
29 Mar 2016 20:21:44.000	611	29999992115.25220
29 Mar 2016 20:21:45.000	612	29999992043.98800
29 Mar 2016 20:21:46.000	613	29999991972.72620
29 Mar 2016 20:21:47.000	614	29999991901.46690
29 Mar 2016 20:21:48.000	615	29999991830.21010
29 Mar 2016 20:21:49.000	616	29999991758.95590
29 Mar 2016 20:21:50.000	617	29999991687.70430
29 Mar 2016 20:21:51.000	618	29999991616.45520
29 Mar 2016 20:21:52.000	619	29999991545.20880
29 Mar 2016 20:21:53.000	620	29999991473.96500

29 Mar 2016 20:21:54.000	621	29999991402.72380
29 Mar 2016 20:21:55.000	622	29999991331.48540
29 Mar 2016 20:21:56.000	623	29999991260.24960
29 Mar 2016 20:21:57.000	624	29999991189.01660
29 Mar 2016 20:21:58.000	625	29999991117.78620
29 Mar 2016 20:21:59.000	626	29999991046.55870
29 Mar 2016 20:22:00.000	627	29999990975.33400
29 Mar 2016 20:22:01.000	628	29999990904.11200
29 Mar 2016 20:22:02.000	629	29999990832.89290
29 Mar 2016 20:22:03.000	630	29999990761.67670
29 Mar 2016 20:22:04.000	631	29999990690.46330
29 Mar 2016 20:22:05.000	632	29999990619.25280
29 Mar 2016 20:22:06.000	633	29999990548.04530
29 Mar 2016 20:22:07.000	634	29999990476.84070
29 Mar 2016 20:22:08.000	635	29999990405.63900
29 Mar 2016 20:22:09.000	636	29999990334.44040
29 Mar 2016 20:22:10.000	637	29999990263.24470
29 Mar 2016 20:22:11.000	638	29999990192.05210
29 Mar 2016 20:22:12.000	639	29999990120.86250
29 Mar 2016 20:22:13.000	640	29999990049.67600
29 Mar 2016 20:22:14.000	641	29999989978.49260
29 Mar 2016 20:22:15.000	642	29999989907.31240
29 Mar 2016 20:22:16.000	643	29999989836.13520
29 Mar 2016 20:22:17.000	644	29999989764.96120
29 Mar 2016 20:22:18.000	645	29999989693.79040
29 Mar 2016 20:22:19.000	646	29999989622.62290
29 Mar 2016 20:22:20.000	647	29999989551.45850

APPENDIX B. MATLAB GEOLOCATION PROGRAM CODE

```
%Program for Geolocation of EMI Emitters by O3b Satellites - Connolly
%*****
%Sec 1. Inputs
%*****
filename = 'ThesisDopShift.xlsx'; %File name for Excel stored STK generated data
sheet = 'Flat30N'; %Sheet Name for Excel Data
ETime=xlsread(filename,sheet,'B3:B303'); %Read data from Excel
YJam=(xlsread(filename,sheet,'C3:C303')); % Read data from Excel
SatInitTime=4293; %STK Scenario Time at Start of EMI recv.
%Beam Center (deg)
lat=30;
%For Error Calculator
ActLat=30;
ActLong=0;
%Sat Longitude at Scenario Start
SatInitLong=-80;
%Time Step for Baseline Rdot Calcs
dt=.01;

%*****
%Sec 2. Constants and Properties
%*****
%mu
mu = 3.986004e14;
%Earth's radii (m)
Re=6378136;
%Oblate Earth
e=.081819301;
ellipsoid=[Re e];
%Sidereal day (s)
sd=86164.1;
%Speed of light (m/s)
c = 3e8;
%Satellite Altitude (m)
Z = 8063e3;
%Semimajor Axis (m)
a=Re+Z;
%Sat. Orbital Period (s)
T = 2*pi*(sqrt(a.^3/mu));
%Relative Angular Velocity of Sat to Earth (rad/s)
RotV=(2*pi)/(T)-(2*pi)/(sd);
```

```

%*****
%Sec 3. Jammer abeam time calculation, centering, plotting
%*****
RawDat=polyfit(ETime, YJam, 3);
Dfreq=polyder(RawDat);
DDfreq=polyder(Dfreq);
AbeamTime=roots(DDfreq);
FnotJam=polyval(RawDat, AbeamTime);
XRaw=-ETime;
TJam=XRaw+AbeamTime; %Center data at t=0
maxTime=max(TJam);
minTime=min(TJam);
RecFreqJam=polyfit(TJam,YJam,3);
figure
plot (TJam, YJam,'--k');
title('Received Freq (Hz) Relative to Satellite Location')
xlabel('Time (s) Relative to Abeam Point')
ylabel('Received Frequency (Hz)')
hold on

YJamFit=polyval(RecFreqJam,TJam);
YJamResid=YJam-YJamFit;
SSresid=sum(YJamResid.^2);
SStotal=(length(YJam)-1)*var(YJam);
rsq=1-SSresid/SStotal;
adj_rsq=1-SSresid/SStotal*(length(YJam)-1)/(length(YJam)-...
    length(RecFreqJam));
XTrackJam=polyval(RecFreqJam,maxTime);

%*****
%Sec. 4. Longitude LOP calculation
%*****
LongEst=SatInitLong+(RotV*(SatInitTime+AbeamTime)*180/pi)

%*****
%Sec 5. Rec. Freq Curves of Sim Emitters for Comparison/Latitude LOP
%*****
Tbase=(minTime:dt:maxTime);
Tdbase=(minTime:dt:(maxTime+dt));
Angle=RotV*Tdbase;

%*****
%Sec. 5.1. Baseline Curve 3.5 deg Below Beam Center
lat1=(lat-3.5)*pi/180; %deg to rad
Nphi1=Re/sqrt(1-e.^2*(sin(lat1)).^2);

```

```

JamPosX1=a*Nphi1*cos(lat1)*cos(Angle);
JamPosY1=Nphi1*cos(lat1)*sin(Angle);
JamPosZ1=(1-e.^2)*Nphi1*sin(lat1);
JamPos1=sqrt(JamPosX1.^2+JamPosY1.^2+JamPosZ1.^2);
Rdot1=(diff(JamPos1))/dt;
Y1=(Rdot1/c)*FnotJam+FnotJam;
plot (Tbase, Y1);
hold on
RecFreq1=polyfit(Tbase,Y1,3);
XTrack1=polyval(RecFreq1,maxTime);
YJamFit1=polyval(RecFreq1,Tbase);
YJamResid1=Y1-YJamFit1;
SSresid1=sum(YJamResid1.^2);
SStotal1=(length(Y1)-1)*var(Y1);
rsq1=1-SSresid1./SStotal1;
adj_rsq1=1-SSresid1./SStotal1*(length(Y1)-1)./(length(Y1)-...
length(RecFreq1));

%*****
%Sec. 5.2. Baseline Curve 3 deg Below Beam Center
lat2=(lat-3)*pi/180; %deg to rad
Nphi2=Re/sqrt(1-e.^2*(sin(lat2)).^2);
JamPosX2=a*Nphi2*cos(lat2)*cos(Angle);
JamPosY2=Nphi2*cos(lat2)*sin(Angle);
JamPosZ2=(1-e.^2)*Nphi2*sin(lat2);
JamPos2=sqrt(JamPosX2.^2+JamPosY2.^2+JamPosZ2.^2);
Rdot2=(diff(JamPos2))/dt;
Y2=(Rdot2/c)*FnotJam+FnotJam;
plot (Tbase, Y2);
hold on
RecFreq2=polyfit(Tbase,Y2,3);
XTrack2=polyval(RecFreq2,maxTime);
YJamFit2=polyval(RecFreq2,Tbase);
YJamResid2=Y2-YJamFit2;
SSresid2=sum(YJamResid2.^2);
SStotal2=(length(Y2)-1)*var(Y2);
rsq2=1-SSresid2./SStotal2;
adj_rsq2=1-SSresid2./SStotal2*(length(Y2)-1)./(length(Y2)-...
length(RecFreq2));

%*****
%Sec. 5.3. Baseline Curve 2.5 deg Below Beam Center
lat3=(lat-2.5)*pi/180; %deg to rad
Nphi3=Re/sqrt(1-e.^2*(sin(lat3)).^2);
JamPosX3=a*Nphi3*cos(lat3)*cos(Angle);

```

```

JamPosY3=Nphi2*cos(lat3)*sin(Angle);
JamPosZ3=(1-e.^2)*Nphi3*sin(lat3);
JamPos3=sqrt(JamPosX3.^2+JamPosY3.^2+JamPosZ3.^2);
Rdot3=(diff(JamPos3))/dt;
Y3=(Rdot3/c)*FnotJam+FnotJam;
plot (Tbase, Y3);
hold on
RecFreq3=polyfit(Tbase,Y3,3);
XTrack3=polyval(RecFreq3,maxTime);
YJamFit3=polyval(RecFreq3,Tbase);
YJamResid3=Y3-YJamFit3;
SSresid3=sum(YJamResid3.^2);
SStotal3=(length(Y3)-1)*var(Y3);
rsq3=1-SSresid3./SStotal3;
adj_rs3=1-SSresid3./SStotal3*(length(Y3)-1)./(length(Y3)-...
    length(RecFreq3));

%*****
%Sec. 5.4. Baseline Curve 2 deg Below Beam Center
lat4=(lat-2)*pi/180; %deg to rad
Nphi4=Re/sqrt(1-e.^2*(sin(lat4)).^2);
JamPosX4=a-Nphi4*cos(lat4)*cos(Angle);
JamPosY4=Nphi2*cos(lat4)*sin(Angle);
JamPosZ4=(1-e.^2)*Nphi4*sin(lat4);
JamPos4=sqrt(JamPosX4.^2+JamPosY4.^2+JamPosZ4.^2);
Rdot4=(diff(JamPos4))/dt;
Y4=(Rdot4/c)*FnotJam+FnotJam;
plot (Tbase, Y4);
hold on
RecFreq4=polyfit(Tbase,Y4,3);
XTrack4=polyval(RecFreq4,maxTime);
YJamFit4=polyval(RecFreq4,Tbase);
YJamResid4=Y4-YJamFit4;
SSresid4=sum(YJamResid4.^2);
SStotal4=(length(Y4)-1)*var(Y4);
rsq4=1-SSresid4./SStotal4;
adj_rs4=1-SSresid4./SStotal4*(length(Y4)-1)./(length(Y4)-...
    length(RecFreq4));

%*****
%Sec. 5.5. Baseline Curve 1.5 deg Below Beam Center
lat5=(lat-1.5)*pi/180; %deg to rad
Nphi5=Re/sqrt(1-e.^2*(sin(lat5)).^2);
JamPosX5=a-Nphi5*cos(lat5)*cos(Angle);
JamPosY5=Nphi2*cos(lat5)*sin(Angle);

```

```

JamPosZ5=(1-e.^2)*Nphi5*sin(lat5);
JamPos5=sqrt(JamPosX5.^2+JamPosY5.^2+JamPosZ5.^2);
Rdot5=(diff(JamPos5))/dt;
Y5=(Rdot5/c)*FnotJam+FnotJam;
plot (Tbase, Y5);
hold on
RecFreq5=polyfit(Tbase,Y5,3);
XTrack5=polyval(RecFreq5,maxTime);
YJamFit5=polyval(RecFreq5,Tbase);
YJamResid5=Y5-YJamFit5;
SSresid5=sum(YJamResid5.^2);
SStotal5=(length(Y5)-1)*var(Y5);
rsq5=1-SSresid5./SStotal5;
adj_rs5=1-SSresid5./SStotal5*(length(Y5)-1)./(length(Y5)-...
length(RecFreq5));

%*****
%Sec. 5.6. Baseline Curve 1 deg Below Beam Center
lat6=(lat-1)*pi/180; %deg to rad
Nphi6=Re/sqrt(1-e.^2*(sin(lat6)).^2);
JamPosX6=a-Nphi6*cos(lat6)*cos(Angle);
JamPosY6=Nphi2*cos(lat6)*sin(Angle);
JamPosZ6=(1-e.^2)*Nphi6*sin(lat6);
JamPos6=sqrt(JamPosX6.^2+JamPosY6.^2+JamPosZ6.^2);
Rdot6=(diff(JamPos6))/dt;
Y6=(Rdot6/c)*FnotJam+FnotJam;
plot (Tbase, Y6);
hold on
RecFreq6=polyfit(Tbase,Y6,3);
XTrack6=polyval(RecFreq6,maxTime);
YJamFit6=polyval(RecFreq6,Tbase);
YJamResid6=Y6-YJamFit6;
SSresid6=sum(YJamResid6.^2);
SStotal6=(length(Y6)-1)*var(Y6);
rsq6=1-SSresid6./SStotal6;
adj_rs6=1-SSresid6./SStotal6*(length(Y6)-1)./(length(Y6)-...
length(RecFreq6));

%*****
%Sec. 5.7. Baseline Curve .5 deg Below Beam Center
lat7=(lat-.5)*pi/180; %deg to rad
Nphi7=Re/sqrt(1-e.^2*(sin(lat7)).^2);
JamPosX7=a-Nphi7*cos(lat7)*cos(Angle);
JamPosY7=Nphi2*cos(lat7)*sin(Angle);
JamPosZ7=(1-e.^2)*Nphi7*sin(lat7);

```

```

JamPos7=sqrt(JamPosX7.^2+JamPosY7.^2+JamPosZ7.^2);
Rdot7=(diff(JamPos7))/dt;
Y7=(Rdot7/c)*FnotJam+FnotJam;
plot (Tbase, Y7);
hold on
RecFreq7=polyfit(Tbase,Y7,3);
XTrack7=polyval(RecFreq7,maxTime);
YJamFit7=polyval(RecFreq7,Tbase);
YJamResid7=Y7-YJamFit7;
SSresid7=sum(YJamResid7.^2);
SStotal7=(length(Y7)-1)*var(Y7);
rsq7=1-SSresid7./SStotal7;
adj_rs7=1-SSresid7./SStotal7*(length(Y7)-1)./(length(Y7)-...
length(RecFreq7));

%*****
%Sec. 5.8. Baseline Curve Beam Center
lat8=(lat)*pi/180; %deg to rad
Nphi8=Re/sqrt(1-e.^2*(sin(lat8)).^2);
JamPosX8=a-Nphi8*cos(lat8)*cos(Angle);
JamPosY8=Nphi8*cos(lat8)*sin(Angle);
JamPosZ8=(1-e.^2)*Nphi8*sin(lat8);
JamPos8=sqrt(JamPosX8.^2+JamPosY8.^2+JamPosZ8.^2);
Rdot8=(diff(JamPos8))/dt;
Y8=(Rdot8/c)*FnotJam+FnotJam;
plot (Tbase, Y8);
hold on
RecFreq8=polyfit(Tbase,Y8,3);
XTrack8=polyval(RecFreq8,maxTime);
YJamFit8=polyval(RecFreq8,Tbase);
YJamResid8=Y8-YJamFit8;
SSresid8=sum(YJamResid8.^2);
SStotal8=(length(Y8)-1)*var(Y8);
rsq8=1-SSresid8./SStotal8;
adj_rs8=1-SSresid8./SStotal8*(length(Y8)-1)./(length(Y8)-...
length(RecFreq8));

%*****
%Sec. 5.9. Baseline Curve .5 deg Above Beam Center
lat9=(lat+.5)*pi/180; %deg to rad
Nphi9=Re/sqrt(1-e.^2*(sin(lat9)).^2);
JamPosX9=a-Nphi9*cos(lat9)*cos(Angle);
JamPosY9=Nphi9*cos(lat9)*sin(Angle);
JamPosZ9=(1-e.^2)*Nphi9*sin(lat9);
JamPos9=sqrt(JamPosX9.^2+JamPosY9.^2+JamPosZ9.^2);

```

```

Rdot9=(diff(JamPos9))/dt;
Y9=(Rdot9/c)*FnotJam+FnotJam;
plot (Tbase, Y9);
hold on
RecFreq9=polyfit(Tbase,Y9,3);
XTrack9=polyval(RecFreq9,maxTime);
YJamFit9=polyval(RecFreq9,Tbase);
YJamResid9=Y9-YJamFit9;
SSresid9=sum(YJamResid9.^2);
SStotal9=(length(Y9)-1)*var(Y9);
rsq9=1-SSresid9./SStotal9;
adj_rs9=1-SSresid9./SStotal9*(length(Y9)-1)./(length(Y9)-...
length(RecFreq9));

%*****
%Sec. 5.10. Baseline Curve 1 deg Above Beam Center
lat10=(lat+1)*pi/180; %deg to rad
Nphi10=Re/sqrt(1-e.^2*(sin(lat10)).^2);
JamPosX10=a-Nphi10*cos(lat10)*cos(Angle);
JamPosY10=Nphi2*cos(lat10)*sin(Angle);
JamPosZ10=(1-e.^2)*Nphi10*sin(lat10);
JamPos10=sqrt(JamPosX10.^2+JamPosY10.^2+JamPosZ10.^2);
Rdot10=(diff(JamPos10))/dt;
Y10=(Rdot10/c)*FnotJam+FnotJam;
plot (Tbase, Y10);
hold on
RecFreq10=polyfit(Tbase,Y10,3);
XTrack10=polyval(RecFreq10,maxTime);
YJamFit10=polyval(RecFreq10,Tbase);
YJamResid10=Y10-YJamFit10;
SSresid10=sum(YJamResid10.^2);
SStotal10=(length(Y10)-1)*var(Y10);
rsq10=1-SSresid10./SStotal10;
adj_rs10=1-SSresid10./SStotal10*(length(Y10)-1)./(length(Y10)-...
length(RecFreq10));

%*****
%Sec. 5.11. Baseline Curve 1.5 deg Above Beam Center
lat11=(lat+1.5)*pi/180; %deg to rad
Nphi11=Re/sqrt(1-e.^2*(sin(lat11)).^2);
JamPosX11=a-Nphi11*cos(lat11)*cos(Angle);
JamPosY11=Nphi2*cos(lat11)*sin(Angle);
JamPosZ11=(1-e.^2)*Nphi11*sin(lat11);
JamPos11=sqrt(JamPosX11.^2+JamPosY11.^2+JamPosZ11.^2);
Rdot11=(diff(JamPos11))/dt;

```

```

Y11=(Rdot11/c)*FnotJam+FnotJam;
plot (Tbase, Y11);
hold on
RecFreq11=polyfit(Tbase,Y11,3);
XTrack11=polyval(RecFreq11,maxTime);
YJamFit11=polyval(RecFreq11,Tbase);
YJamResid11=Y11-YJamFit11;
SSresid11=sum(YJamResid11.^2);
SStotal11=(length(Y11)-1)*var(Y11);
rsq11=1-SSresid11./SStotal11;
adj_rsq11=1-SSresid11./SStotal11*(length(Y11)-1)./(length(Y11)-...
    length(RecFreq11));

%*****
%Sec. 5.12. Baseline Curve 2 deg Above Beam Center
lat12=(lat+2)*pi/180; %deg to rad
Nphi12=Re/sqrt(1-e.^2*(sin(lat12)).^2);
JamPosX12=a-Nphi12*cos(lat12)*cos(Angle);
JamPosY12=Nphi12*cos(lat12)*sin(Angle);
JamPosZ12=(1-e.^2)*Nphi12*sin(lat12);
JamPos12=sqrt(JamPosX12.^2+JamPosY12.^2+JamPosZ12.^2);
Rdot12=(diff(JamPos12))/dt;
Y12=(Rdot12/c)*FnotJam+FnotJam;
plot (Tbase, Y12);
hold on
RecFreq12=polyfit(Tbase,Y12,3);
XTrack12=polyval(RecFreq12,maxTime);
YJamFit12=polyval(RecFreq12,Tbase);
YJamResid12=Y12-YJamFit12;
SSresid12=sum(YJamResid12.^2);
SStotal12=(length(Y12)-1)*var(Y12);
rsq12=1-SSresid12./SStotal12;
adj_rsq12=1-SSresid12./SStotal12*(length(Y12)-1)./(length(Y12)-...
    length(RecFreq12));

%*****
%Sec. 5.13. Baseline Curve 2.5 deg Above Beam Center
lat13=(lat+2.5)*pi/180; %deg to rad
Nphi13=Re/sqrt(1-e.^2*(sin(lat13)).^2);
JamPosX13=a-Nphi13*cos(lat13)*cos(Angle);
JamPosY13=Nphi13*cos(lat13)*sin(Angle);
JamPosZ13=(1-e.^2)*Nphi13*sin(lat13);
JamPos13=sqrt(JamPosX13.^2+JamPosY13.^2+JamPosZ13.^2);
Rdot13=(diff(JamPos13))/dt;
Y13=(Rdot13/c)*FnotJam+FnotJam;

```

```

plot (Tbase, Y13);
hold on
RecFreq13=polyfit(Tbase,Y13,3);
XTrack13=polyval(RecFreq13,maxTime);
YJamFit13=polyval(RecFreq13,Tbase);
YJamResid13=Y13-YJamFit13;
SSresid13=sum(YJamResid13.^2);
SStotal13=(length(Y13)-1)*var(Y13);
rsq13=1-SSresid13./SStotal13;
adj_rs13=1-SSresid13./SStotal13*(length(Y13)-1)./(length(Y13)-...
length(RecFreq13));

%*****
%Sec. 5.14. Baseline Curve 3 deg Above Beam Center
lat14=(lat+3)*pi/180; %deg to rad
Nphi14=Re/sqrt(1-e.^2*(sin(lat14)).^2);
JamPosX14=a-Nphi14*cos(lat14)*cos(Angle);
JamPosY14=Nphi14*cos(lat14)*sin(Angle);
JamPosZ14=(1-e.^2)*Nphi14*sin(lat14);
JamPos14=sqrt(JamPosX14.^2+JamPosY14.^2+JamPosZ14.^2);
Rdot14=(diff(JamPos14))/dt;
Y14=(Rdot14/c)*FnotJam+FnotJam;
plot (Tbase, Y14);
hold on
RecFreq14=polyfit(Tbase,Y14,3);
XTrack14=polyval(RecFreq14,maxTime);
YJamFit14=polyval(RecFreq14,Tbase);
YJamResid14=Y14-YJamFit14;
SSresid14=sum(YJamResid14.^2);
SStotal14=(length(Y14)-1)*var(Y14);
rsq14=1-SSresid14./SStotal14;
adj_rs14=1-SSresid14./SStotal14*(length(Y14)-1)./(length(Y14)-...
length(RecFreq14));

%*****
%Sec. 5.15. Baseline Curve 3.5 deg Above Beam Center
lat15=(lat+3.5)*pi/180; %deg to rad
Nphi15=Re/sqrt(1-e.^2*(sin(lat15)).^2);
JamPosX15=a-Nphi15*cos(lat15)*cos(Angle);
JamPosY15=Nphi15*cos(lat15)*sin(Angle);
JamPosZ15=(1-e.^2)*Nphi15*sin(lat15);
JamPos15=sqrt(JamPosX15.^2+JamPosY15.^2+JamPosZ15.^2);
Rdot15=(diff(JamPos15))/dt;
Y15=(Rdot15/c)*FnotJam+FnotJam;
plot (Tbase, Y15);

```

```

hold on
RecFreq15=polyfit(Tbase,Y15,3);
XTrack15=polyval(RecFreq15,maxTime);
YJamFit15=polyval(RecFreq15,Tbase);
YJamResid15=Y15-YJamFit15;
SSresid15=sum(YJamResid15.^2);
SStotal15=(length(Y15)-1)*var(Y15);
rsq15=1-SSresid15./SStotal15;
adj_rsq15=1-SSresid15./SStotal15*(length(Y15)-1)./(length(Y15)-...
length(RecFreq15));

legend Jam -3.5deg -3deg -2.5deg -2deg -1.5deg -1deg -.5deg BeamCenter...
+.5deg +1deg +1.5deg +2deg +2.5deg +3deg +3.5deg;
hold off

%*****
%Sec. 6. Interpolation of Jammer Latitude from Base Curves
%*****
YT=[lat1 lat2 lat3 lat4 lat5 lat6 lat7 lat8 lat9 lat10 lat11 lat12 lat13...
lat14 lat15];
XT=[XTrack1 XTrack2 XTrack3 XTrack4 XTrack5 XTrack6 XTrack7 XTrack8...
XTrack9 XTrack10 XTrack11 XTrack12 XTrack13 XTrack14 XTrack15];
XTSolve=polyfit(XT,YT,4);
XTrkFit=polyval(XTSolve,XT);
XTrkResid=YT-XTrkFit;
SSresidXT=sum(XTrkResid.^2);
SStotalXT=(length(YT)-1)*var(YT);
rsqXT=1-SSresidXT./SStotalXT;
adj_rsqXT=1-SSresidXT./SStotalXT*(length(YT)-1)./(length(YT)-...
length(XTSolve));
%figure
%plot (XT, YT);
hold off
LatRad=polyval(XTSolve,XTrackJam); %Latitude in radians
LatEst=LatRad*180/pi %radians to degrees

%*****
%Sec. 7. Display Estimated Position on Map (Red X)
%*****
figure
axesm eckert4;
framem; gridm;
axis on
geoshow('landareas.shp','Facecolor','y');
linem(LatEst,LongEst,'LineStyle','none','LineWidth',2,'Color','r',...

```

```

    'Marker','x','MarkerSize',10);
hold on

%*****
%Sec. 8. Calculate Error from Actual Position
%*****
[LatDist]=distance(ActLat, ActLong, LatEst, ActLong, ellipsoid)/1000 %km
[LongDist]=distance(ActLat, ActLong,ActLat, LongEst, ellipsoid)/1000 %km
[Dist]=distance(ActLat, ActLong, LatEst, LongEst, ellipsoid)/1000 %km

%*****
%Sec. 9. Longitude Error Correction/Plot Based on Obtained results (Red +)
%*****
EWErr=[-1.485 -2.838 -5.900 -10.931];
lats=[15 30 45 60];
EWCorfit=polyfit(lats, EWErr, 2);
EWCor=polyval(EWCorfit, LatEst);
LongCor=SatInitLong+(RotV*(SatInitTime+AbeamTime)*180/pi)-(EWCor*RotV*...
    180/pi)+.0649
[LongCorDist]=distance(ActLat, ActLong, ActLat, LongCor, ellipsoid)/1000 %km
[CorDist]=distance(ActLat, ActLong, LatEst, LongCor, ellipsoid)/1000 %km
linem(LatEst,LongCor,'LineStyle','none','LineWidth',2,'Color','r',...
    'Marker','+','MarkerSize',10);
hold on

%*****
%Sec. 10. Plot Actual Location on Map for Comparison (Green X)
%*****
linem(ActLat,ActLong,'LineStyle','none','LineWidth',2,'Color','g',...
    'Marker','X','MarkerSize',10);
hold off

```

THIS PAGE INTENTIONALLY LEFT BLANK

LIST OF REFERENCES

- Amundson, Isaac, Janos Sallai, Xenofon Koutsoukos, and Akos Ledeczi. "Radio Interferometric Angle of Arrival Estimation." In *Proceedings of 2010 European Conference on Wireless Sensor Networks*. Coimbra, Portugal: Springer, 2010.
- Blumenthal, Steven H. "Medium Earth Orbit Ka Band Satellite Communications System." In *MILCOM 2013 - 2013 IEEE Military Communications Conference*. San Diego: IEEE, 2013. 273-277.
- Carlson, A. Bruce, and Paul B. Crilly. *Communication Systems: An Introduction to Signals and Noise in Electrical Communications* (5th. ed.). New York: McGraw-Hill, 2011.
- C-Com Satellite Systems Inc. Ka-Band. (accessed May 17, 2016). <http://www.c-comsat.com/solutions/ka-band/>.
- Chow, Tina L. "Passive Emitter Location Using Digital Terrain Data." Master's thesis, Binghamton: Binghamton University of State University of New York, 2001.
- Curlander, John C., and Robert N. McDonough. *Synthetic Aperture Radar Systems and Signal Processing*. New York: John Wiley & Sons, 1991.
- Fredrick, Brian C. "Geolocation of Source Interference From A Single Satellite With Multiple Antennas." Master's thesis, Monterey: Naval Postgraduate School, 2014.
- Frontline Communications. Mobile Ka-Band Solution Debuts for Satellite Newsgathering. August 21, 2013. <http://www.frontlinecomm.com/news/KaWriteUp.pdf>.
- Government Accountability Office. *Defense Satellite Communications: DOD Needs Additional Information to Improve Procurements*. (GAO-15-459). Washington, DC: Government Accountability Office, 2015.
- "Joint Spectrum Interference Resolution (JSIR) Procedures." *Chairman of the Joint Chiefs of Staff Manual (CJCSM 3320.02D)*. June 3, 2013.
- Larson, Wiley J., and James R. Wertz. *Space Mission Analysis and Design* (3rd. ed.). Hawthorne, CA: Microcosm Press, 1999.
- Loomis, Herschel H. *Geolocation of Electromagnetic Emitters* (Rev. 2007). (NPS-EC-00-003). Monterey: Naval Postgraduate School, 1999.
- Musicki, Darko, and Wolfgang Koch. "Geolocation using TDOA and FDOA Measurements." In *Proceedings of the 11th International Conference on Information Fusion*. Cologne, Germany: IEEE, 2008. 1987-1994.

- O3b Networks. "O3b Government USG Bulletin." O3bNetworks.com. July 16, 2015.
http://www.o3bnetworks.com/wp-content/uploads/2015/08/USG-Bulletin_16JUL15.pdf.
- Sargent, Anne-Wainscott. "Fighting Satellite Interference on All Fronts." Via Satellite - SatelliteToday.com. March 1, 2013.
<http://www.satellitetoday.com/publications/via-satellite-magazine/features/2013/03/01/fighting-satellite-interference-on-all-fronts/>.
- Skylogic. NEWSPOTTER. (accessed May 17, 2016).
http://www.skylogic.it/?page_id=2309&lang=en.
- Whalen, David G. "Communications Satellites Short History." NASA History Division. November 30, 2010. <http://history.nasa.gov/satcomhistory.html>.
- Wilgenbusch, Ronald C., and Alan Heisig. "Command and Control Vulnerabilities to Communications Jamming." *Joint Forces Quarterly*, no. 69 (April 2013): 56-63.
- Williams, Richard A., and Heywood I. Paul. "Potential Uses of the Military Ka-band for Wideband MILSATCOM Systems." In *Military Communications Conference*. Boston: IEEE, 1998. 30-34.
- Witzgall, Hanna. "A Reliable Doppler-Based Solution for Single Sensor Geolocation." In *IEEE Aerospace Conference*. Big Sky: IEEE, 2013.

INITIAL DISTRIBUTION LIST

1. Defense Technical Information Center
Ft. Belvoir, Virginia
2. Dudley Knox Library
Naval Postgraduate School
Monterey, California